IMPLEMENTATION AND PERFORMANCE ANALYSIS OF THE DVB-T STANDARD SYSTEM

A THESIS SUBMITTED TO
THE GRADUATE SCHOOL OF NATURAL AND APPLIED SCIENCES
OF
MIDDLE EAST TECHNICAL UNIVERSITY

BY

MEHMET YÜKSEKKAYA

IN THE PARTIAL FULFILLMENT OF THE REQUIREMENTS
FOR
THE DEGREE OF MASTER OF SCIENCE
IN
ELECTRICAL AND ELECTRONICS ENGINEERING

NOVEMBER 2005

Approval of the Graduate School of Natural and Applied Sciences

_____

Prof. Dr. Canan Özgen

Director

I certify that this thesis satisfies all the requirements as a thesis for the degree of Master of Science

_____

Prof. Dr. İsmet Erkmen

Head of Department

This is to certify that we have read this thesis and that in our opinion it is fully adequate, in scope and quality, as a thesis for the degree of Master of Science.

_____

Assoc. Prof. Dr. T. Engin Tuncer

Supervisor

Examining Committee Members

Assoc. Prof. Dr. Aydın Alatan (METU,EE) _____

Assoc. Prof. Dr. T. Engin Tuncer (METU,EE) _____

Asst. Prof. Dr. Yeşim Serinağaoğlu (METU,EE) _____

Asst. Prof. Dr. Özgür Yılmaz (METU,EE) _____

Asst. Prof. Dr. Aysel Şafak (BAŞKENT UNIVERSITY,EE) _____

I hereby declare that all information in this document has been obtained and presented in accordance with academic rules and ethical conduct. I also declare that, as required by these rules and conduct, I have fully cited and referenced all material and results that are not original to this work.

Name, Last name : Mehmet YÜKSEKKAYA

Signature :

ABSTRACT

IMPLEMENTATION AND PERFORMANCE ANALYSIS OF THE DVB-T STANDARD SYSTEM

Yüksekkaya, Mehmet

M.S., Department of Electrical and Electronics Engineering

Supervisor: Assoc. Prof. Dr. T. Engin Tuncer

November 2005, 94 pages

Terrestrial Digital Video Broadcasting (DVB-T) is a standard for wireless broadcast of MPEG-2 video. DVB-T is based on channel coding algorithms and uses Orthogonal Frequency Division Multiplexing (OFDM) as a modulation scheme.

In this thesis, we have implemented the standard of ETSI EN 300 744 for Digital Video Broadcasting in MATLAB. This system is composed of the certain blocks which include OFDM modulation, channel estimation, channel equalization, frame synchronization, error-protection coding, to name a few of such blocks. We have investigated the performance of the complete system for different wireless broadcast impairments. In this performance analysis, we have considered Rayleigh fading multi-path channels with Doppler shift and framing synchronization errors and obtained the bit error rate (BER), and channel minimum square error performances versus different maximum Doppler shift

values, different channel equalization techniques and different channel estimation algorithms.

Furthermore, we have investigated different interpolations methods for the interpolation of channel response.

It is shown that minimum mean-square error (MMSE) type equalization has a better performance in symbol estimation compared to zero forcing (ZF) equalizer. Also linear interpolation in time and low pass frequency interpolation, for time frequency interpolation of channel response can be used for practical application.

Keywords: DVB-T, OFDM, channel estimation, channel equalization, frame synchronization, error-protection coding

ÖZ

DVB-T STANDART SİSTEMİNİN GERÇEKLEŞTİRİLMESİ VE BAŞARIM İNCELEMELERİNİN YAPILMASI

Yüksekkaya, Mehmet

Yüksek Lisans, Elektrik ve Elektronik Mühendisliği Bölümü

Tez Yöneticisi: Doç. Dr. T. Engin Tuncer

Kasım 2005, 94 sayfa

Karasal, Sayısal Görüntü Yayını (DVB-T), MPEG-2 görüntülerinin kablosuz yayını belirleyen bir standarttır. DVB-T kanal kodlama çözüm yollarına dayanır ve Dikgen Frekans Bölüşümlü Çoklama (OFDM) tekniğini kipleme için kullanır.

Bu tezde, Sayısal Görüntü Yayını (DVB) standartı olan ETSI EN 300 744'ü MATLAB bilgisayar programı üzerinde gerçekledik. Bu sistem belli başlı bloklardan oluşur, bu bloklardan birkaçı isimlendirilirse bunlar, OFDM kiplemesi, kanal tahmini, kanal eşitlemesi, çerçeve eşzamanlaması ve hatalardan korunma kodlamasıdır. Bütün sistemin başarımını çeşitli kablosuz yayın sorunları için inceledik. Bu başarım incelemelerinde, Doppler kaymasını içeren Rayleigh sönümlü çok-yollu kanallarını, ve çerçeve eş zamanlaması hatalarını göz önünde bulundurduk, ikil hata oranına (BER) ve kanalın en düşük karesel hata (MSE) oranına karşılık çeşitli Doppler kayma değerlerinin, çeşitli kanal eşitleme

tekniklerinin ve çeşitli kanal tahmini çözüm yollarının başarım sonuçlarını elde ettik.

Ayrıca, kanal tepkisinin aradeğerlenmesi için farklı aradeğerleme metotlarını inceledik.

En az ortalama kare eşitleme tipinin sıfır tazyikleme eşitlemesine göre sembol kestiriminin başarımının daya iyi olduğunu gösterildi. Bununla beraber pratik uygulamalarda kanal tepkisinin zaman frekans aradeğerlemesi için zamanda doğrusal ve frekansta alçak geçiren aradeğerlenme kullanılabilir.

Anahtar kelimeler: DVB-T, OFDM, kanal tahmini, kanal eşitlemesi, çerçeve eşzamanlaması, hatalardan korunma kodlaması

To My Family

ACKNOWLEDGEMENTS

I wish to express my deepest thanks and gratitude to my supervisor, Assoc. Prof. Dr. T. Engin Tuncer, for his invaluable guidance, encouragement, enthusiasm, and extra-ordinary patience.

I wish to thank to Tübitak-BAYG, for the scholarship they provided me for my thesis work.

I would also like to thank Asst. Prof. Dr. Aysel Şafak for her suggestions and comments.

Thanks to my friends Uygar Karadeniz and Murat Özsüt for their friendship and motivation.

Thanks to my colleagues in Başkent University Biomedical Engineering Department for their great encouragement and continuous moral support.

Finally, I would like to thank to my parents, my sister and my brother for their continued support, encouragement, and sacrifice through the years, and I will be forever indebted to them for all that they have done.

TABLE OF CONTENTS

LIST OF TABLES

LIST OF FIGURES

LIST OF ABBREVIATIONS

AWGN	Additive White Gaussian Noise
BER	Bit Error Rate
CTF	Channel Transfer Function's
CP	Cyclic Prefix
DAB	Digital Audio Broadcasting
DFT	Discrete Fourier Transform
ETSI	European Telecommunications Standards Institute
FFT	Fast Fourier Transform
FDM	Frequency Division Multiplexing
HDTV	High-Definition TeleVision
ICI	Inter Carrier Interference
ISI	Inter Symbol Interference
IFFT	Inverse Fast Fourier Transform
LS	Least Square
LMMSE	Linear Minimum Mean Square error
ML	Maximum Likelihood
MMSE	Minimum Mean-Square Error
MC	Multicarrier Communication
N	Number of Sub-Carriers
OFDM	Orthogonal Frequency Division Multiplexing
PAR	Peak-To-Average Ratio
RS	Reed Solomon
SFN	Single Frequency Network
DVB-T	Terrestrial Digital Video Broadcasting
TPS	Transmission Parameter Signaling
WLAN	Wireless Local Area Network
ZF	Zero-Forcing

CHAPTER 1

INTRODUCTION

The ETSI ETS 300 744 standard describes a baseline transmission system for Digital Terrestrial Television Broadcasting. It specifies the error correction coding and modulation system intended for Digital TV terrestrial services. DVB-T uses Orthogonal Frequency Division Multiplexing (OFDM) as a modulation scheme.

The main objective of this thesis is implementing the DVB-T standard system with all functional blocks, and then evaluating performance analysis for different approaches advised to clarify the impairments due to broadcasting effects. It is chosen to investigate DVB-T because it is a dominant next generation standard for wireless broadcast of MPEG-2 video [1] and today many digital television specifications are introduced by DVB Project.

Basically two types of modes are being used in DVB-T; these modes are 2k and 8k mode. In 2k mode number of sub-carriers is 2048 whereas it is 8192 in the 8k mode. The 2K non-hierarchical DVB-T is implemented with the transmitter and receiver systems.

The transmitter system consists of energy dispersal, outer coder (RS coder), inner coder (Convolutional coder), inner and outer interleavers, mapper, frame adaptation, OFDM modulator and guard interval functional blocks. For the receiver system frame synchronization, guard interval removal, OFDM demodulator, channel estimation and equalization, frame extraction, demapper

inner and outer deinterleavers, Viterbi decoder, outer decoder (RS decoder) and energy dispersal removal functional blocks are implemented.

By these functional blocks a complete DVB-T simulation system is formed. Using this DVB-T simulation system some of the important aspects of DVB-T and OFDM usage in DVB-T are examined and compared. These important issues for DVB-T system are error correction coding, pilot power allocation, pilot positions, DVB-T frame architecture, channel estimation, channel equalization, interpolation usage for channel estimation, frame synchronization. Simulation results are provided for AWGN, Rayleigh and Rician channel using Doppler Effect and frame synchronization error.

Four Types of channel estimation are investigated, least square (LS) estimation, linear minimum mean square error (LMMSE) estimation with known channel transfer function, linear minimum mean square error estimation with utilizing the result of LS estimation and minimum mean square error (MMSE) estimation with the assumption of noise to be white and its variance is known. The implemented channel estimation process also includes different types of interpolation techniques such as; linear, low pass, Spline, DFT interpolations.

To recover the transmitted symbols using estimated channel, channel equalization is performed by zero-forcing (ZF) and minimum mean-square error (MMSE) techniques.

Frame synchronizer uses maximum likelihood (ML) frame synchronization algorithm which is based on the periodicity of OFDM frames provided by cyclic prefix.

We have compared the performances of these algorithms by the means of bit error rate, channel mean square error rate and framing offset with AWGN, multi-path Rayleigh fading and Rician fading channels.

In the following chapters firstly, the DVB-T standard is discussed considering frame architecture, error correction coding and modulation schemes

which are formed the transmitter architecture also in this chapter a receiver is defined. The receiver architecture is not mentioned in the standard [1], it is left as an open issue in order to support the different approaches for developments, so a basic receiver model is also proposed in this chapter. The second chapter concentrates on OFDM which is defined as a multicarrier transmission technique based on dividing the available spectrum into many carriers which are modulated by a low rate data stream. In the following chapter the channel estimation and equalization processes are discussed with the detailed performance analysis then the frame synchronization is explained. Finally the conclusions derived from the literature survey and results obtained from simulations are restated and compared.

CHAPTER 2

TERRESTRIAL DIGITAL VIDEO BROADCASTING (DVB-T) SYSTEM

2.1 INTRODUCTION

Digital broadcasting is the delivery of broadcasting services via the transmission of graphical data and sound data on what is known as the digital highway. EN 300 744 standard [1] is introduced by European Telecommunications Standards Institute (ETSI) and it describes a baseline system for terrestrial transmission of digital television signals. The standard gives a general description of only the transmitter part for digital terrestrial TV. In this chapter we will discuss the transmitter and a receiver model for 2K non-hierarchical mode of DVB-T. First the DVB-T Transmitter then DVB-T Receiver is explained.

2.2 DVB-T TRANSMITTER

The transmitter system is defined as the functional block of equipment performing the adaptation of the MPEG-2 data stream to the base-band terrestrial TV signal. The main steps of this adaptation are:

- Energy dispersal by scrambling;
- Outer coding and outer interleaving;
- Inner coding and inner interleaving;
- Mapping and Frame adaptation;

§ OFDM transmission.

The elements of the transmitter will be explained on the basis of a block diagram in Figure 2.1 [1].

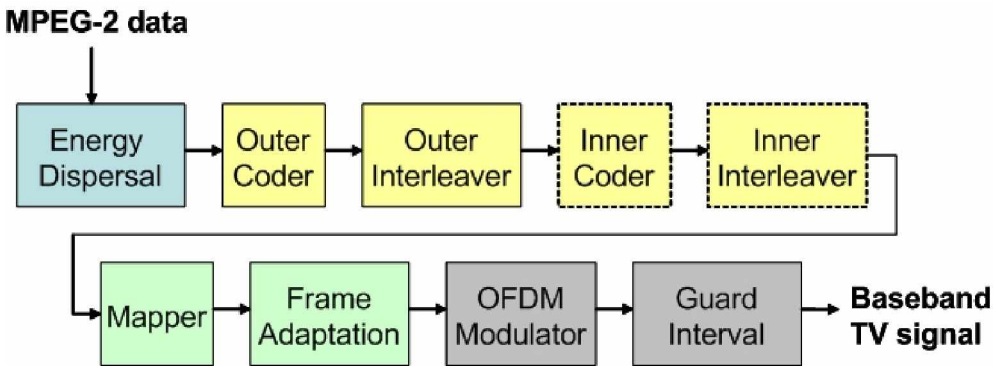

Figure 2.1: Transmitter block Diagram

2.2.1 Energy Dispersal

Energy dispersal is used to achieve the most evenly distributed power-density spectrum possible. In energy dispersal the signals are combined bitwise with the output stream of a pseudo-random generator via an "exclusive-or" operation as shown in figure 2.2.[1]

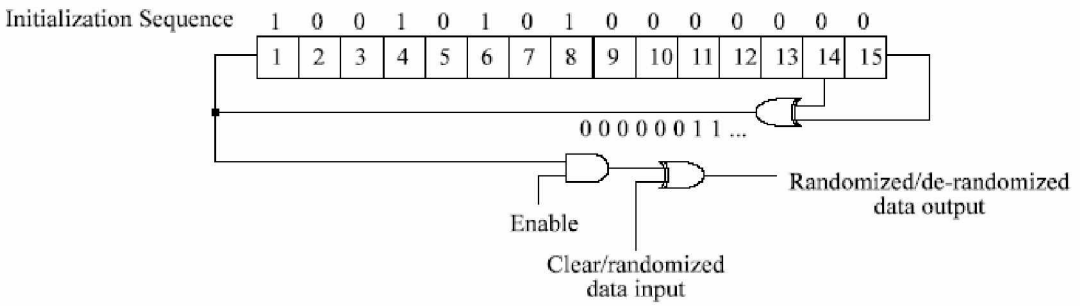

Figure 2.2: Diagram of energy dispersal circuit

2.2.2 Outer Coder

Outer coder is a Reed Solomon (RS) encoder, which adds 16 correction bytes to each block of 188 bytes so a total 204 bytes of code forms.

This Reed Solomon block code allows to correct up to 8 random erroneous bytes in a received word of 204 bytes in the receiver.

2.2.3 Outer Inter-Leaver

In order to correct long burst errors in addition to bit errors and short burst errors, an interleaver is inserted between the outer and the inner coder [2]. The interleaver supplies no additional error correction code, it rearranges the symbols generated by the outer coder. The interleaver is a convolutional interleaver with an interleaving depth of I=12. The base delay is M=17, and therefore the block length of the interleaver is n=I*M=204 bytes which is a RS code [1], [2].

2.2.4 Inner Coder

Inner coder is a convolutional encoder with code rate of R=1/2 and generator polynomials $G_1=171_{OCT}$, $G_2 = 133_{OCT}$ as in Figure 2.3. This code is used to produce several punctured codes with different coding rates.

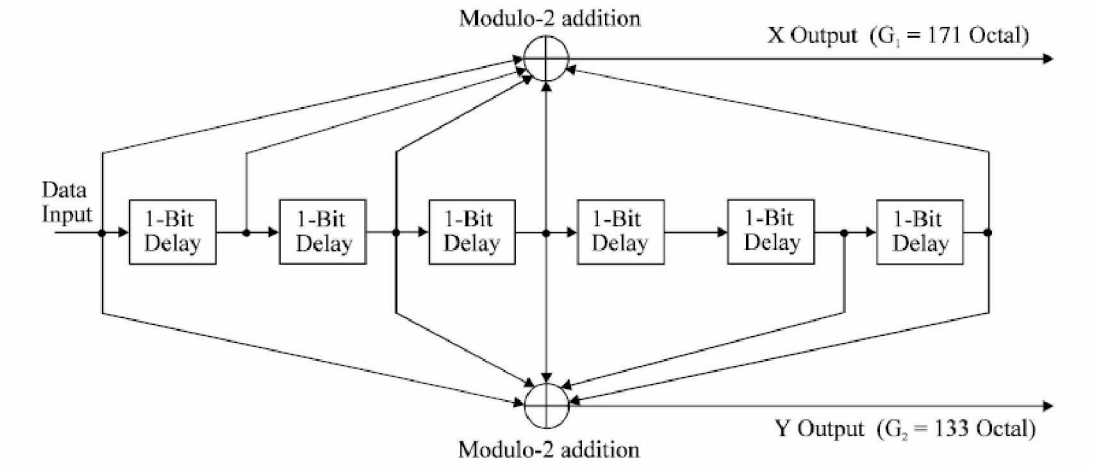

Figure 2.3: Structure of the convolutional encoder

The puncturing is used because one of the disadvantages of convolutional codes is the low code rate (R=1/2). This means that twice as many bits transferred that the actual information would require. By puncturing, the code rate can be increased, which of course increase the correction requirements. Puncturing is omitting some of the bits in an order as shown in Table 2.1 [1], [2].

Table 2.1: Puncturing patterns for the given convolutional encoder.

Code Rates r	Puncturing pattern	Transmitted sequence (after parallel-to-serial conversion)
1/2	X: 1 Y: 1	$X_1 Y_1$
2/3	X: 1 0 Y: 1 1	$X_1 Y_1 Y_2$
3/4	X: 1 0 1 Y: 1 1 0	$X_1 Y_1 Y_2 X_3$
5/6	X: 1 0 1 0 1 Y: 1 1 0 1 0	$X_1 Y_1 Y_2 X_3 Y_4 X_5$
7/8	X: 1 0 0 0 1 0 1 Y: 1 1 1 1 0 1 0	$X_1 Y_1 Y_2 Y_3 Y_4 X_5 Y_6 X_7$

2.2.5 Inner Inter-leaver

DVB-T uses OFDM as a modulation scheme. OFDM is a multi-carrier technique which is the distribution of successive data over the large number of available carriers and used to minimize the effects of frequency-selective impairments. By inner interleaving the disturbances, affecting individual neighboring carriers can be dispersed in other words inner-interleaving is a frequency interleaving which can disperse long sequence of corrupted bits at the receiver. Inner interleaving consists of bit-wise interleaving followed by symbol interleaving. The inner interleaver supplies no additional error correction code as in outer interleaver, it rearranges the symbols generated by the inner coder. Data come from inner coder demultiplexed into sub-stream after that bit-wise interleaving takes place then the data are formed to symbols and symbol interleaving takes place as shown in Figure 2.4. The details of demultiplexing, bit-wise interleaving and symbol interleaving are described in the EN 300 744 standard [1].

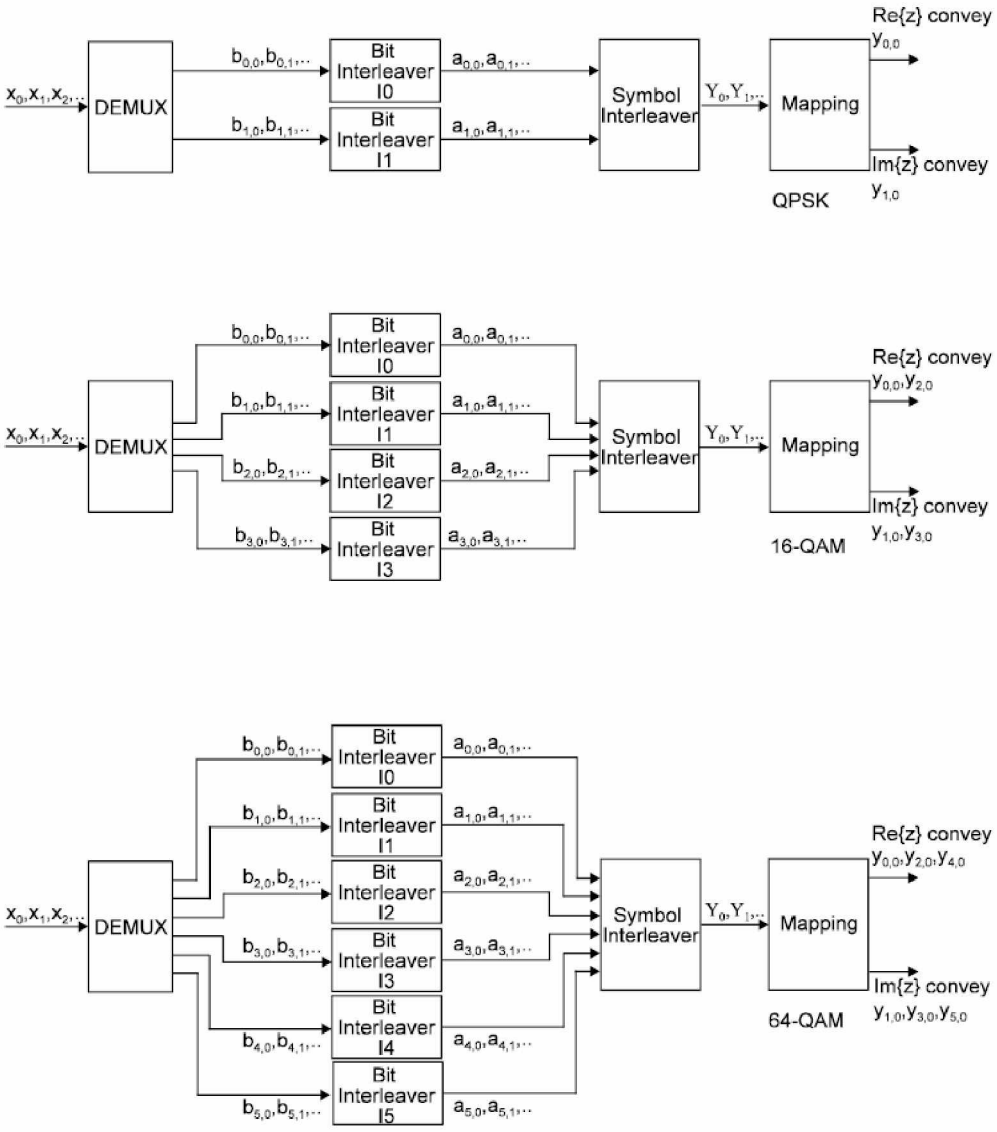

Figure 2.4: Structure of inner interleaver and mapping of symbols.

2.2.6 MAPPER

The useful data on the individual carriers of OFDM symbol are formed of complex values which are the mapped form of bits. There are 3 alternatives of mapping scheme in non-hierarchical mode DVB-T which are QPSK, 16-QAM, and 64-QAM. The required constellation of corresponding mapping is defined in standard [1] and given in Figure 2.5.

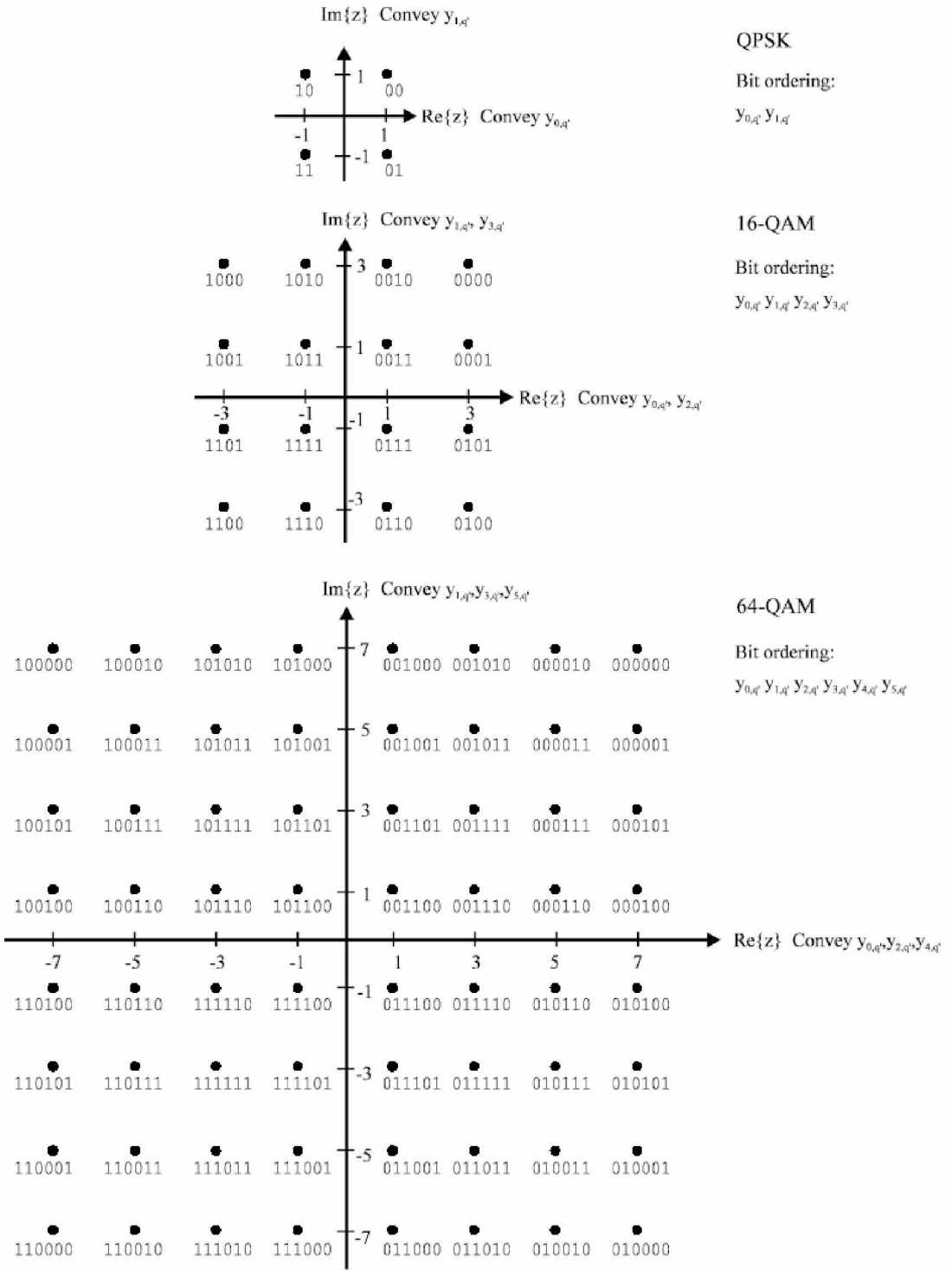

Figure 2.5: The QPSK, 16-QAM and 64-QAM mappings and the corresponding bit patterns.

2.2.7 Frame Adaptation

The transmitted signal is organized in frames, and each frame consists of 68 OFDM symbols. Four frames constitute one super-frame. Each symbol is constitute by a set of K=6817 carriers in 8K mode an K=1705 carriers in 2K mode. All symbols contain data and reference information. In addition to the transmitted data an OFDM frame contains:

- Scattered pilot cells;
- Continual pilot cells;
- Transmission Parameter Signaling (TPS) carriers.

The pilots can be used for frequency synchronization, frame synchronization, time synchronization, channel estimation, transmission mode identification and can be used to follow the phase noise. The TPS carriers are used to give information about parameters of transmission scheme.

Each OFDM frames conveys 68 TPS bits and each OFDM symbols conveys one TPS bit. The TPS carriers carried information about mapping scheme, hierarchy information, guard interval size, inner coder rates, transmission modes, frame number in a super-frame and cell identifier.

Scattered and continual pilot cells are modulated according to a PRBS sequence generator in Figure 2.6 and their transmitted value is known by the receiver. These cells are transmitted in boosted power levels.

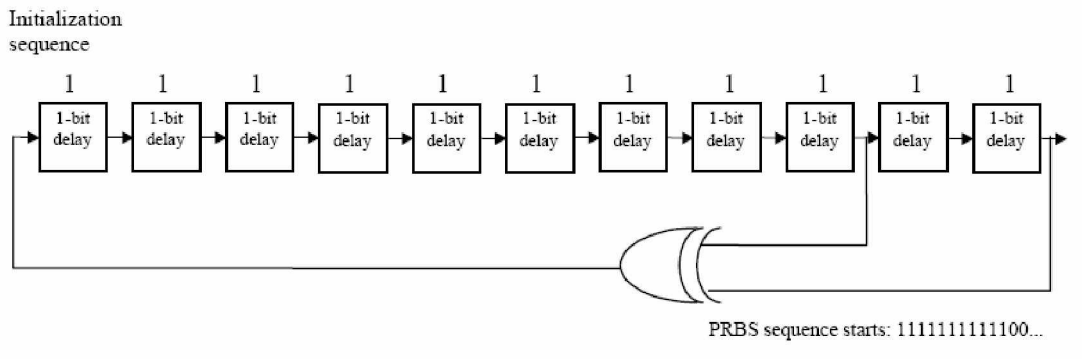

Figure 2.6: Generation of PRBS for pilot cells

The location of continual pilot cells and TPS carriers are given in Table 2.2, 2.3 in order. The scattered pilots are scattered over the transmission frame according to a plan which shown in Figure 2.7 [1].

Table 2.2: Continual pilot positions in an OFDM symbol for 2K mode.

2K mode						
0	48	54	87	141	156	192
201	255	279	282	333	432	450
483	525	531	618	636	714	759
765	780	804	873	888	918	939
942	969	984	1 050	1 101	1 107	1 110
1 137	1 140	1 146	1 206	1 269	1 323	1 377
1 491	1 683	1 704				

Table 2.3: TPS carrier positions in an OFDM symbol for 2K mode.

2K mode				
34	50	209	346	413
569	595	688	790	901
1 073	1 219	1 262	1 286	1 469
1 594	1 687			

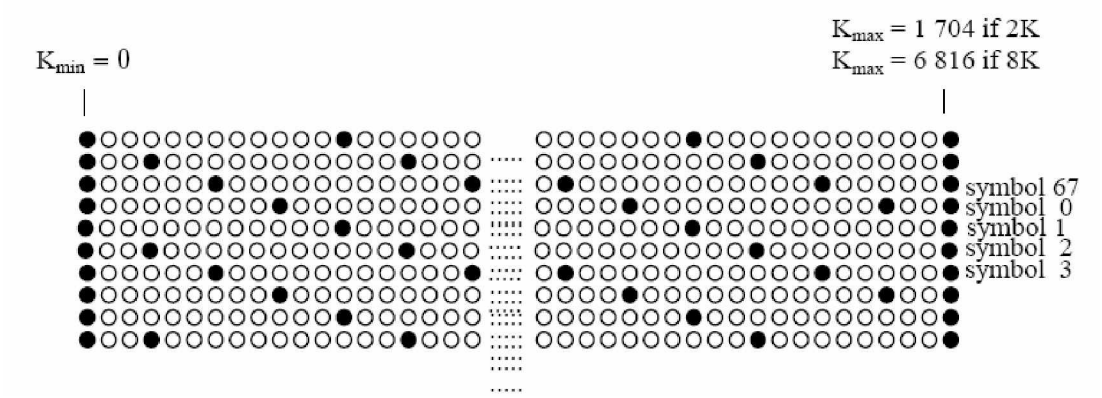

Figure 2.7: Frame structure, scattered pilots are the black filled circles.

2.2.8 OFDM

Orthogonal Frequency Division Multiplexing (OFDM) is a special case of multi-carrier transmission technique in which available frequency spectrum is divided into many closely spaced sub-carriers. The idea behind these sub-carriers is to transform a very high data rate into a set of very low data rates that are then transmitted in parallel and by different frequencies. In this sense, OFDM is similar to FDMA because in FDMA the bandwidth is divided into many channels, so that, in a multi-user environment, each channel is allocated to a user. The difference is the carriers chosen in OFDM are much more closely spaced than in FDMA (1 kHz in OFDM as opposed to about 30 kHz in FDMA) this

increases the efficiency of spectrum usage. In order to appropriately choosing the frequency spacing between carriers they are made orthogonal to each other. OFDM is discussed in chapter 3 in detail.

2.3 DVB-T RECEIVER

In the receiver side of the DVB-T system in addition with the error correction decoding block, de-mapper, and OFDM demodulator, receiver includes some enhancement blocks to clarify wireless channel impairments. Wireless channel is characterized by: path loss; multi-path delay spread, fading characteristic, Doppler spread, Co-channel and adjacent channel interference. According to these impairments of wireless channel receiver mainly consists of OFDM demodulator, frame synchronization, channel estimation and channel equalization, and error correction decoding blocks. DVB-T receiver architecture is given in Figure 2.8

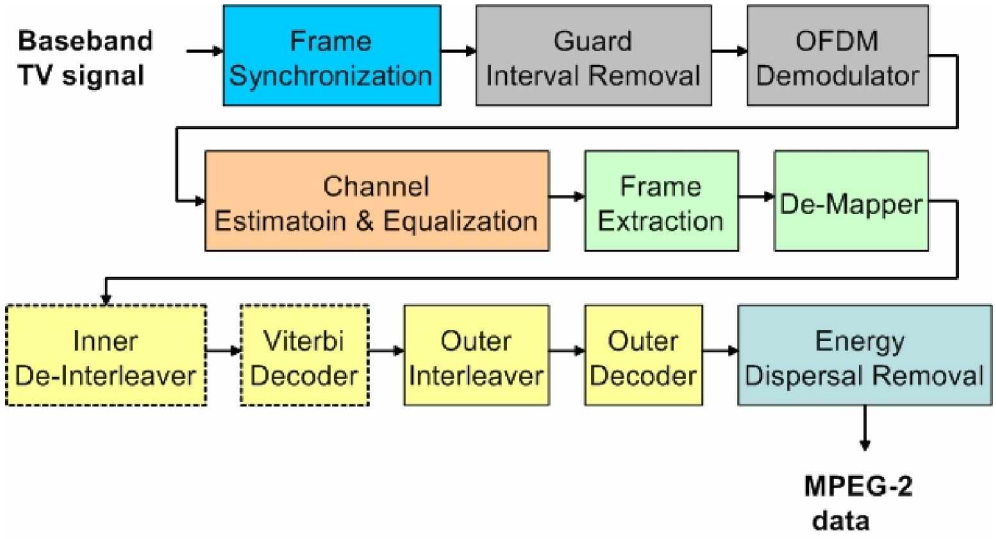

Figure 2.8: Receiver Block Diagram

2.3.1 Frame Synchronization

In typical communication system one of the problems is to detect a frame in the received signal to realize coding, block processing etc. To compensate framing error frame synchronization must be performed. We investigate Maximum Likelihood (ML) Frame Synchronization technique in chapter 5.

2.3.2 Channel Estimation

In order to estimate the channel several channel estimation algorithms based on pilots are implemented. Also three types of interpolation algorithms which are linear, low-pass, and DFT are investigated. These processes are discussed in chapter 4 in detail.

2.3.3 Channel Equalization

After the channel is estimated, equalization can be done; two types of channel equalizations ZF and MMSE are investigated and discussed also in chapter 4.

2.3.4 Error Correction Decoding

A concatenated channel decoding scheme with de-mapping and de-interleaving are used in the error correction decoding part. The de-mapping block is the inverse of mapping block but it generates soft decision information for convolutional encoder, soft decision is preferred because it improves the error correction capability. After de-mapping block as an inverse of inner interleaver we have inner de-interleaver, it performs symbol and bit de-interleaving respectively and is used to avoid long sequence of corrupted bits at the inner decoder.

At the transmitter side puncturing is applied to the convolutional coded data so between inner de-interleaver and inner decoder de-puncturing is performed. De-puncturing is inserting dummy soft decisions to the proper positions and so restoring the necessary rate 1/2 to convolutional encoder. In the inner decoder part Viterbi decoder as a decoder of convolutional encoder is used. The main important parameter of Viterbi algorithm except the parameters, which also used in the convolutional encoder, is the number soft decision bits. Increasing soft decision bit number improves the error-correction capability. As shown is [2] a resolution higher than 3 is an hardly improvement and only increase the implementation requirement. However, 4 bits soft decision is rarely used in implementations.

The DVB-T standard uses a convolutional code of rate R=1/2 with constraint length of K=7. In this way it is possible to achieve a bit-error rate of less then $2.4*10^{-4}$ at the output of the Viterbi decoder with sufficient SNR and this is the ratio corresponds to maximum permissible bit error rate at the input of RS (204,188) decoder, then the bit error rate at the output of the RS decoder is less than $1*10^{-11}$ is obtained which is the quasi error free rate.

2.4 ADDITIONAL FEATURES FOR DVB

The two main development trends based on DVB is DVB-H and DVB-RCT. DVB-H technology adapts the DVB-T system for digital terrestrial television to the specific requirements of handheld, battery-powered receivers. DVB-H can provide a downstream channel at high data rates which can be used standalone or as an enhancement of mobile telecoms networks which many typical handheld terminals are able to access anyway [3]. Time slicing technology is employed in order to reduce power consumption for small handheld terminals.

IP datagrams are transmitted as data bursts in small time slots. The front end of the receiver switches on only for the time interval when the data burst of a

selected service is on air. Within this short period of time a high data rate is received which can be stored in a buffer.

With the advent of DVB-H, there are significant challenges for the systems which underlie DVB broadcast services. Amongst the issues are the harmonisation of service discovery and selection, purchase and protection between the broadcast and the mobile telecommunications worlds. In the IP world of DVB-H, such issues need to build upon the stability of the broadcast world, and embrace the successful methods of the telecommunications world. If there are 30 DVB-H services available, one will need to ensure that there are appropriate electronic programme guidelines and service protection arrangements. In November 2005 DVB finalised a set of specifications for the IP datacasting domain which will be published by ETSI at the beginning of 2006.

DVB-RCT (Return Channel Terrestrial) is intended to provide standard specification for interactivity in the UHF/VHF bands. Using the newly defined DVB-RCT standard [4] as a companion of the world-wide proven, recognized and adopted Terrestrial DVB system, DVB-T is no longer limited to unidirectional broadcast and it can become a true Terrestrial Wireless Interactive system. The DVB-RCT technical subgroup performed a tremendous work to define the physical layer (RCT-PHY), the Medium Access Control layer (RCT-MAC) and the RF Implementation Guidelines. As a result, the DVB-RCT standard makes use of a Multiple Access OFDM arrangement, to constitute a high bandwidth Wireless Interactive Terrestrial Digital TV system.

CHAPTER 3

ORTHOGONAL FREQUENCY DIVISION MULTIPLEXING

3.1 Introduction

Orthogonal Frequency Division Multiplexing (OFDM) is defined as a multicarrier transmission technique, which is based on dividing the available spectrum into many carriers which are modulated by a low rate data stream [5], [6], [7].

This chapter starts with giving a brief history of OFDM, after that the ancestors techniques from which the OFDM is evolved are explained, the basic concepts of OFDM technique are discussed next, followed by the explanation of continuous-time and discrete-time OFDM system models, and finally the chapter ends by giving the advantages and disadvantages of the OFDM systems.

3.2 History of OFDM

OFDM history dates back up to the Second World War. OFDM had been used by US military in several high frequency military systems such as KINEPLEX, ANDEFT and KATHRYN [8].

The first US patent on OFDM is filed in 1970 by Robert W. Chang after he outlined a theoretical way to transmit simultaneous data stream trough linear band limited channel without Inter Symbol Interference (ISI) and Inter Carrier Interference (ICI) in 1966 [6]. Around the same time, Saltzberg performed an analysis of the performance of the OFDM system [9].

In 1971, Weinstein and Ebert used Discrete Fourier Transform (DFT) to perform base-band modulation and demodulation therefore the need for a bank of subcarrier oscillators is eliminated [10].

Peled and Ruiz introduced Cyclic Prefix (CP) or cyclic extension in 1980. This solved the problem of maintaining orthogonal characteristics of the transmitted signals at severe transmission conditions [11].

In the 1990s, OFDM was exploited for wideband data communications over mobile radio FM channels, High-bit-rate Digital Subscriber Lines, Asymmetric Digital Subscriber Lines and Very-high-speed Digital Subscriber Lines [12].

Digital Audio Broadcasting (DAB) was the first commercial use of OFDM technology. DAB services came to reality in 1995 in UK and Sweden. The development of Digital Video Broadcasting (DVB) along with High-Definition TeleVision (HDTV) terrestrial broadcasting standard was published in 1995 [12].

Several Wireless Local Area Network (WLAN) standards adopted OFDM on their physical layers (HiperLAN, HiperLAN/2, 802.11a).

Nowadays OFDM is a competitor for future 4th Generations (4G) wireless systems which are expected to emerge by the year 2010 and if OFDM gain prominence in this arena, then it will become the technology of choice in most wireless links worldwide [13].

3.3 Ancestors of OFDM

OFDM is evolved from other basic communication techniques, namely Frequency Division Multiplexing (FDM) and Multicarrier Communications (MC) [14], [15].

3.3.1 Frequency Division Multiplexing (FDM)

Frequency Division Multiplexing (FDM) has been used for a long time to carry more than one signal over a telephone line. The idea behind FDM is the usage of different frequency channels in order to carry different information contents. These channels are identified by their center frequencies of sub frequencies. In order to guarantee the non overlapping frequency separation of adjacent channels, a guard band is left between the sub frequencies. One of the main drawbacks of this approach is the inefficiencies caused by these guard bands. In early days when the digital filtering capabilities are not adequate for sharp filtering of adjacent channels, the designers are forced to leave large frequency guard bands between the sub frequencies.

3.3.2 Multicarrier Communications (MC)

Multicarrier communication concept resembles the FDM technology with the difference that in this concept the communication is between a single data source and a single receiver. The purpose of multicarrier communications is to increase the overall throughput.

Since the operation of multiplexing implies the addition of signals together, referring to MC as FDM is misleading. In MC, a signal is splitted into a number of signals that are modulated over their own frequency channel. These different frequency channels are then multiplexed together as similar to FDM. This is followed by the feeding of the received signals into a demultiplexer that

feeds the different frequency channels to different receivers. Finally, data output of the receivers are combined to form the received signal.

3.4 Orthogonal Frequency Division Multiplexing (OFDM)

Orthogonal Frequency Division Multiplexing (OFDM) is a special case of multicarrier transmission technique in which the available frequency spectrum is divided into many closely spaced sub-carriers that are orthogonal to each other. The idea behind these sub-carriers is to transform a very high data rate into a set of very low data rates that are then transmitted in parallel and by different frequencies.

In this context the term orthogonal means that the signals are totally independent. This is achieved by placing the carriers exactly at the nulls in the modulation spectra of each other. By using orthogonality, sufficient separation in available frequency band is obtained.

In OFDM the data of each carrier overlaps the data in the adjacent ones. This situation of overlapping is actually one of the main factors in the spectral efficiency in OFDM. Another factor in the spectral efficiency of OFDM is the fact that the drop-off of the signal at the band is primarily due to a single carrier which is carrying a low data rate. In Figure 3.1 spectra of individual sub-carriers are illustrated [7].

OFDM systems are also very efficient for the way they handle inter symbol interference (ISI). ISI is diminished as a result of the modulation of each sub-carrier at a very low symbol rate, which causes the symbols to be much longer than the channel impulse response. [7]

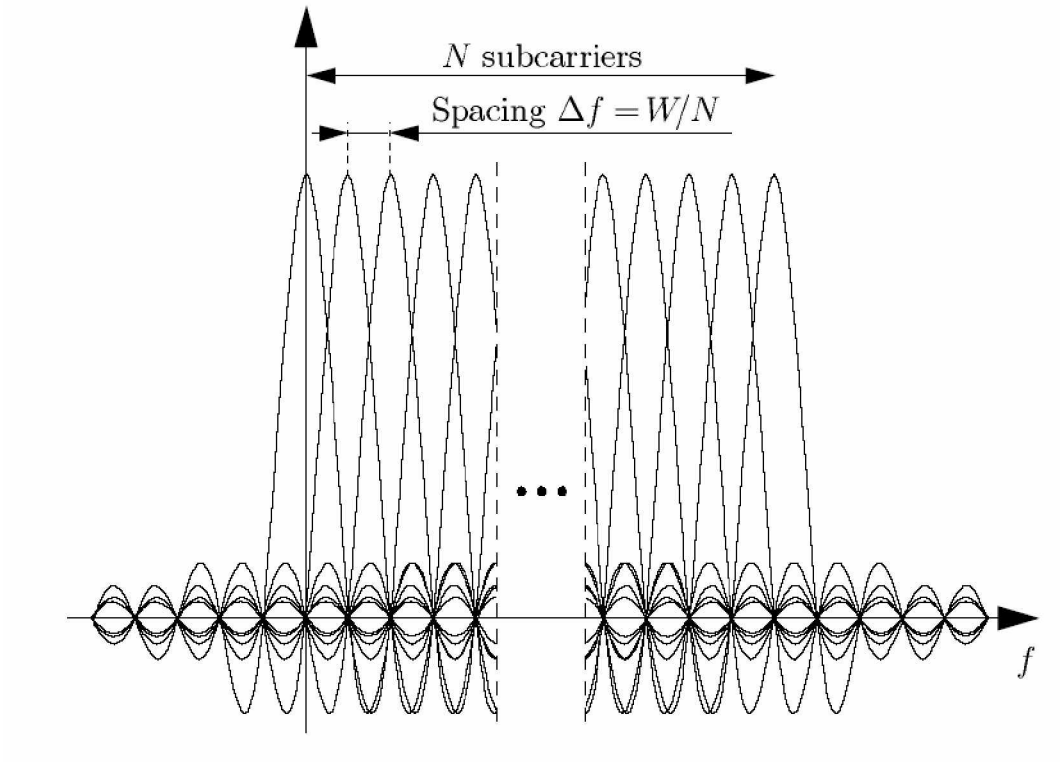

Figure 3.1: Spectra of individual sub-carriers over a bandwidth W.

Inverse Fast Fourier Transform (IFFT) and Fast Fourier Transform (FFT) algorithms are used in the modulation and demodulation of the signal in an OFDM system. The time span of the IFFT / FFT vector is chosen much larger than the maximum delay time of echoes in the received multipath signal in order to increase the resistance of the system to multipath channel errors.

3.4.1 Guard Time and Cyclic Extension

The effects of ISI can be completely eliminated by inserting a guard interval between consecutive OFDM symbols. This guard interval must be longer than the multipath delay such that multi-path components from one symbol cannot interfere with the next symbol. Since large numbers of sub-carriers are

used, a total high data rate can be achieved although each sub-carrier operates at a low data rate.

If the guard time is left empty, this may lead to inter-carrier interference (ICI), since the carriers are no longer orthogonal to each other. To avoid this situation, the OFDM symbol is cyclically extended. A cyclic prefix is a copy of the last part of the OFDM symbol, which is inserted to the beginning of he transmitted symbol as shown in Figure 3.2 [7]. By this method, the transmitted signal becomes periodic without affecting the orthogonality of the carriers.

This ensures that the delayed replicas of the OFDM symbols always have an integer number of cycles within the FFT interval as long as the multi-path delay spread is less than the guard time [7].

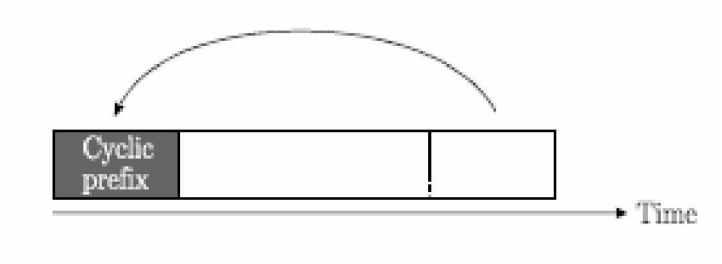

Figure 3.2: The cyclic prefix.

3.4.2 OFDM Generation

The block diagram of a discrete-time OFDM system is given in Figure 3.3. OFDM is generated by firstly choosing the spectrum required, based on the input data, and modulation scheme used. Each carrier to be produced is assigned some data to transmit. The required amplitude and phase of the carrier is then calculated based on the modulation scheme (typically differential BPSK, QPSK,

or QAM). Then, the IFFT converts this spectrum into a time domain signal. The FFT transforms a cyclic time domain signal into its equivalent frequency spectrum. The amplitude and phase of the sinusoidal components represent the frequency spectrum of the time domain signal [7].

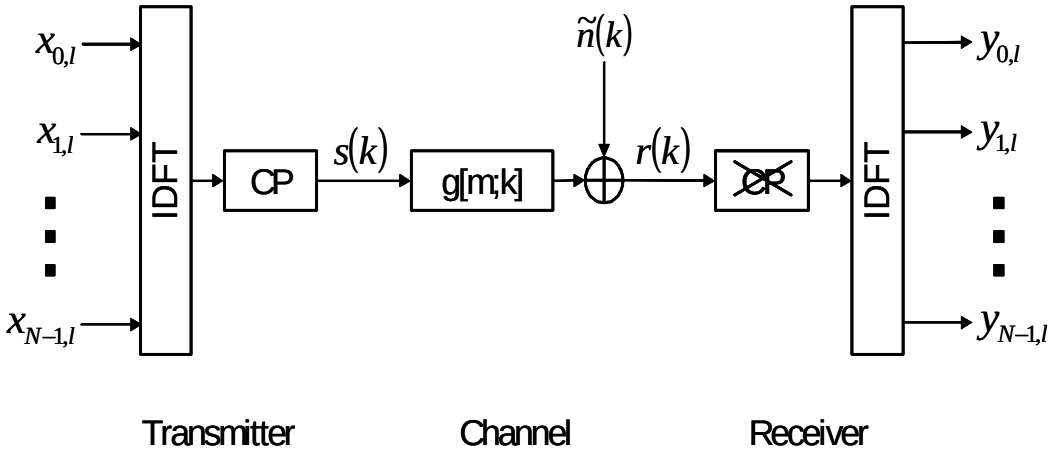

Figure 3.3: Discrete-time base-band OFDM system model.

3.5 Continuous-time OFDM system model

Continuous-time base-band OFDM system model is given in Figure 3.4. Since the early OFDM systems did not utilize digital modulation and demodulation, this model can be considered as the ideal OFDM system which in practice is digitally synthesized. The components of this model will be explained in the following sections.

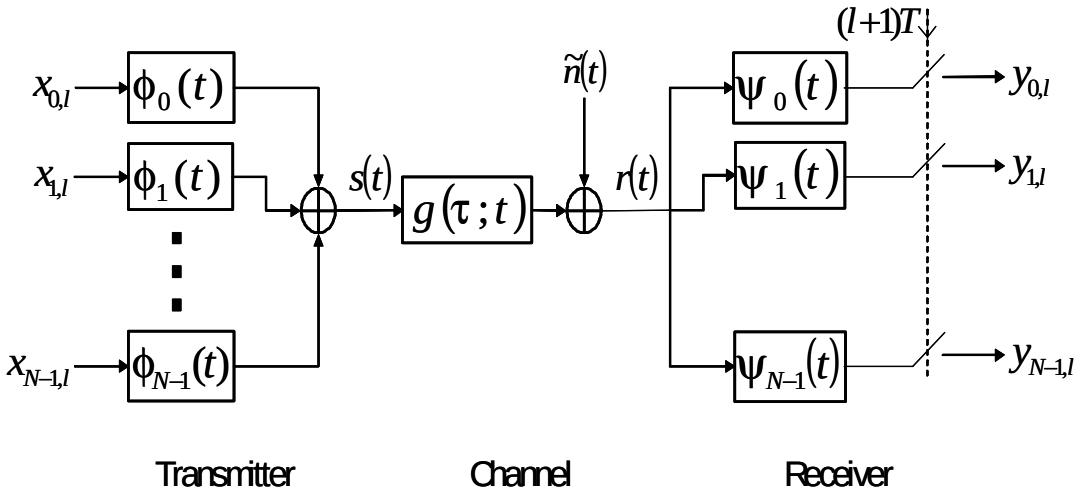

Figure 3.4: Continuous-time base-band OFDM system model.

3.5.1 Transmitter

The transmitter waveforms are given in equation 3.1 where N is the number of carriers in the system, W is the bandwidth in Hertz, T and T_{cp} are the symbol length and cyclic prefix length in seconds respectively.

$$\phi_k(t) = \begin{cases} \frac{1}{\sqrt{T - T_{cp}}} e^{j2\pi \frac{W}{N} k (t - T_{cp})} & \forall t \in [0, T] \\ 0 & otherwise \end{cases} \tag{3.1}$$

In equation 3.1, $T = N/W + T_{cp}$. Also one can notice that $\phi_k(t) = \phi_k(t + N/W)$ when t is within the cyclic prefix $[0, T_{cp}]$. Since $\phi_k(t)$ is a rectangular pulse modulated on the carrier frequency kW/N, it can be said that the OFDM is a technique with N sub-carriers, each carrying a low bit-rate [7].

The waveforms $\phi_k(t)$ are used in the modulation and the expression for the transmitted base-band signal for OFDM symbol number l can be given as,

$$s_l(t) = \sum_{k=0}^{k=N-1} x_{k,l}\phi_k(t - lT) \tag{3.2}$$

In equation 3.2, $x_{0,l}$, $x_{1,l}$, … , $x_{N-1,l}$ are complex numbers obtained from a set of signal constellation points. In the case of an infinite sequence of OFDM symbols are transmitted, the output of the transmitter is a juxtaposition of individual OFDM symbols and can be expressed as,

$$s(t) = \sum_{l=-\infty}^{\infty} s_l(t) = \sum_{l=-\infty}^{\infty}\sum_{k=0}^{N-1} x_{k,l}\phi_k(t - lT) \tag{3.3}$$

3.5.2 Physical channel

Under the assumption of the support of the impulse response $g(\tau;t)$ of the physical channel is restricted to the interval $\tau \in [0,T_{cp}]$, the expression for the received signal becomes, [7]

$$r(t) = (g * s)(t) = \int_0^{T_{cp}} g(\tau;t)s(t-\tau)d\tau + n(t) \tag{3.4}$$

In the previous expression n(t) is the additive, white and complex Gaussian noise.

3.5.3 Receiver

A filter bank which is matched to the last part [T_{cp},T] of the transmitter waveforms $\phi_k(t)$ forms the OFDM receiver. Therefore,

$$\psi_k(t) = \begin{cases} \phi_k^*(T-t) & \forall t \in [0, T-T_p] \\ 0 & otherwise \end{cases} \tag{3.5}$$

It can be seen from equation 3.5 that the cyclic prefix is removed in the receiver. This causes the sampled output from the receiver filter bank to contain no ISI since the cyclic prefix contains all ISI from the previous symbol. Therefore the time index l can be ignored and by using equations 3.3, 3.4 and 3.5, the sampled output at the k^{th} matched filter can be written as,

$$\begin{aligned} y_k &= (r * \psi_k)(t)\,|_{t=T} = \int_{-\infty}^{\infty} r(t)\psi_k(T-t)dt \\ &= \int_{T_{cp}}^{T}\left(\int_0^{T_{cp}} g(\tau;t)\left[\sum_{k'=0}^{N-1} x_{k'}\phi_{k'}(t-\tau)\right]d\tau \right)\phi_k^*(t)dt + \int_{T_{cp}}^{T} \tilde{n}(T-t)\phi_k^*(t)dt \end{aligned} \tag{3.6}$$

The above expression can be simplified by considering the channel to be fixed over the OFDM symbol interval, therefore by denoting the channel as g(t) it can be rewritten as,

$$y_k = \sum_{k'=0}^{N-1} x_{k'} \int_{T_{cp}}^{T}\left(\int_0^{T_{cp}} g(t)\phi_{k'}(t-\tau)d\tau \right)\phi_k^*(t)dt + \int_{T_{cp}}^{T} \tilde{n}(T-t)\phi_k^*(t)dt \tag{3.7}$$

The integration intervals for the above expression implies that $0< t - \tau < T$ therefore the inner integral can be written as,

$$\int_0^{T_{cp}} g(t)\phi_{k'}(t-\tau)d\tau = \int_0^{T_{cp}} g(\tau)\frac{e^{j2\pi k'(t-\tau-T_{cp})W/N}}{\sqrt{T-T_{cp}}}d\tau$$
$$= \frac{e^{j2\pi k'(t-T_{cp})W/N}}{\sqrt{T-T_{cp}}}\int_0^{T_{cp}} g(\tau)e^{-j2\pi k'\tau W/N}d\tau, \qquad T_{cp} < t < T \tag{3.8}$$

The latter part of equation 3.8 is the sampled frequency response of the channel at the k'^{th} subcarrier frequency $f = k'W/N$ and by denoting G(f) as the Fourier transform of $g(\tau)$, it can be written as,

$$h_{k'} = G\left(k'\frac{W}{N}\right) = \int_0^{T_{cp}} g(\tau)e^{-j2\pi k'\tau W/N}d\tau \tag{3.9}$$

Using equation 3.9, the output from the receiver filter bank can be written as,

$$y_k = \sum_{k'=0}^{N-1} x_{k'}\int_{T_{cp}}^{T}\frac{e^{j2\pi k'(t-T_{cp})W/N}}{\sqrt{T-T_{cp}}}h_{k'}\phi_k^*(t)dt + \int_{T_{cp}}^{T}\tilde{n}(T-t)\phi_k^*(t)dt$$
$$= \sum_{k'=0}^{N-1} x_{k'}h_{k'}\int_{T_{cp}}^{T}\phi_{k'}(t)\phi_k^*(t)dt + n_k \tag{3.10}$$
$$where \quad n_k = \int_{T_{cp}}^{T}\tilde{n}(T-t)\phi_k^*(t)dt$$

The transmitter filters $\phi_k(t)$ are orthogonal therefore,

$$\int_{T_{cp}}^{T} \phi_{k'}(t)\phi_k^*(t)dt = \int_{T_{cp}}^{T} \frac{e^{j2\pi k'(t-T_{cp})W/N}}{\sqrt{T-T_{cp}}} \frac{e^{-j2\pi k(t-T_{cp})W/N}}{\sqrt{T-T_{cp}}} dt = \delta[k-k'] \qquad (3.11)$$

In equation 3.11 δ[k] is the Kronecker delta function. It is now possible to simplify equation 3.10 to obtain,

$$y_k = h_k x_k + n_k \qquad (3.12)$$

where n_k is additive white Gaussian noise (AWGN)

It must be noted that while the expressions for the received and sampled signals stay the same, the transmitted energy increases with the length of the cyclic prefix. The transmitted energy per sub-carrier can be expressed as,

$$\int |\phi_k(t)|^2 dt = T/(T-T_{cp}) \qquad (3.13)$$

The cyclic prefix is discarded in the receiver, therefore by denoting the relative length of the cyclic prefix as γ, the expression for the loss in SNR can be given as,

$$SNR_{loss} = -10\log_{10}(1-\gamma) \qquad (3.14)$$

where $\gamma = T_{cp} / T$

From the above equation it is clear that as the cyclic prefix becomes longer, the loss in SNR becomes larger. But in practice, the relative length of the cyclic prefix is small therefore loss in SNR is generally less than 1 dB for $\gamma < 0.2$. As explained previously, since the cyclic prefix acts as a guard space while

maintaining the orthogonality of the sub-carriers, it avoids both ISI and ICI. Therefore ISI and ICI free transmission motivates the small SNR loss [7].

3.6 Discrete-time OFDM system model

Discrete-time model of an OFDM system is previously illustrated in Figure 3.3. As can be seen from this figure, the modulation and demodulation in continuous-model are replaced by IDFT and DFT, respectively. Also the channel is a discrete-time convolution and all integrals are replaced with sums.

Linear convolution in the channel is transformed into a cyclic convolution if the cyclic prefix is chosen longer that the channel. Therefore by denoting cyclic convolution as $\otimes$, N received data points as y_l, N transmitted constellation points as x_l, the channel impulse response (padded with zeroes to obtain a length, N) as g and the uncorrelated Gaussian noise as n_l, the whole OFDM system can be written as, [7]

$$\begin{aligned} y_l &= DFT\left(IDFT\left(x_l\right)\otimes g_l + \tilde{n}_l\right) \\ &= DFT\left(IDFT\left(x_l\right)\otimes g_l\right) + n_l \end{aligned} \tag{3.15}$$

Since the DFT of two cyclically convolved signals is equivalent to the product of their individual DFTs, by denoting h_l as the frequency response of the channel, the above expression can be written as,

$$y_l = x_l \cdot DFT\left(g_l\right) + n_l = x_l \cdot h_l + n_l \tag{3.16}$$

where $h_l = DFT(g_l)$

3.7 Advantages of OFDM

OFDM has many inherent advantages for communication applications. These advantages are listed in the subsequent paragraphs.

OFDM is very effective against the ISI caused due to multi-path delay spread since there is an N (number of sub-carriers) times increase in the symbol time of the OFDM signal. Additionally, by utilizing cyclic extension, ISI can completely eliminated in OFDM.

In digital communication systems another reason for ISI is the lack of amplitude flatness in the frequency response of the channel. However in OFDM systems, since the bandwidth of each sub-carrier is very small, the amplitude response over this narrow bandwidth will be basically flat, making OFDM systems effective against channel distortion.

The use of sub-carrier modulation improves the flexibility of OFDM to channel fading and distortion, and makes it possible for the system to transmit at maximum possible capacity using a technique called channel loading which is based on channel estimation techniques, therefore enabling throughput maximization.

OFDM systems are inherently robust against impulse noise which is generally an effect of atmospheric phenomena such as lightning. Since the symbol duration of an OFDM signal is much larger than that of the corresponding single-carrier system, it is less likely that impulse noise might cause symbol errors.

Also frequency diversity is inherently present in OFDM systems [8], [12].

3.8 Disadvantages of OFDM

Although OFDM has many advantages, it has also a few disadvantages that must be solved [7], [8], and [12].

Since the OFDM signal can be considered as a complex modulated signal at different frequencies, in some cases the signal components add up in phase to produce a large output, or in some may cancel out each other producing zero output. Therefore OFDM transmissions have a high peak-to-average ratio (PAR). There are several techniques such as clipping are utilized to deal with this issue of OFDM.

Another important issue in OFDM transmission is the synchronization. In OFDM systems in order to minimize ICI and ISI, the receiver has to estimate the symbol boundaries and the optimal timing instants. Also the receiver has to estimate and make corrections on the received for the carrier frequency offset; otherwise the orthogonality of the sub-carriers will be lost since the transmitter and receiver use different frequencies. Additionally, if coherent demodulation is used, phase information must be recovered. In order to achieve synchronization in OFDM systems several synchronization methods such as cyclic extension synchronization are utilized.

CHAPTER 4

CHANNEL ESTIMATION AND EQUALIZATION

Wireless communication system performances are also dependent to the radio channel. Channel impairments such as multi-path reflections, path loss, additive noise and Doppler Effect can have a significant impact on the bit error rate. These channel effects in wireless systems must be corrected.

In mobile OFDM case, radio channel are normally frequency selective and time invariant and data are modulated on frequency domain sub-carriers. These modulated data are scaled by different channel frequency response coefficients after passing through the channel. For an accurate communication these channel frequency coefficients on sub-channels are needed. So channel estimation and equalization are necessary for signal correction. The high data rate transmission in OFDM is achieved by using higher order constellations, for robust and coherent detection of such OFDM signals needs accurate channel estimation. The structure of OFDM allows a channel estimation in both time and frequency correlation. In coherent OFDM, channel estimation usually performed by using pilot tones, based on inserting known sub-carriers in the time-frequency direction. In block type training symbol, pilot tones assigned to all sub-carriers in an specific OFDM symbol while, in combinational type pilot aided symbol, pilot tones are uniformly distributed within an OFDM symbol and data tones are assigned to other sub-carriers [16].

In DVB-T OFDM pilot symbols are used to estimate the channel frequency response coefficients and pilot sub-carriers are scattered in OFDM symbols like comb-type pilot aided symbol [17], [18].

In this chapter, various channel estimation and equalization methods are investigated and performance analyses are evaluated in the context of European DVB-T OFDM system the performance results are given in the name of minimum square error (MSE) of channel transfer function, un-coded bit error rate (BER) and coded BER of information.

4.1 OFDM Base-band System Model

For an investigation of channel estimation we consider the OFDM base-band system as depicted in figure 4.1.

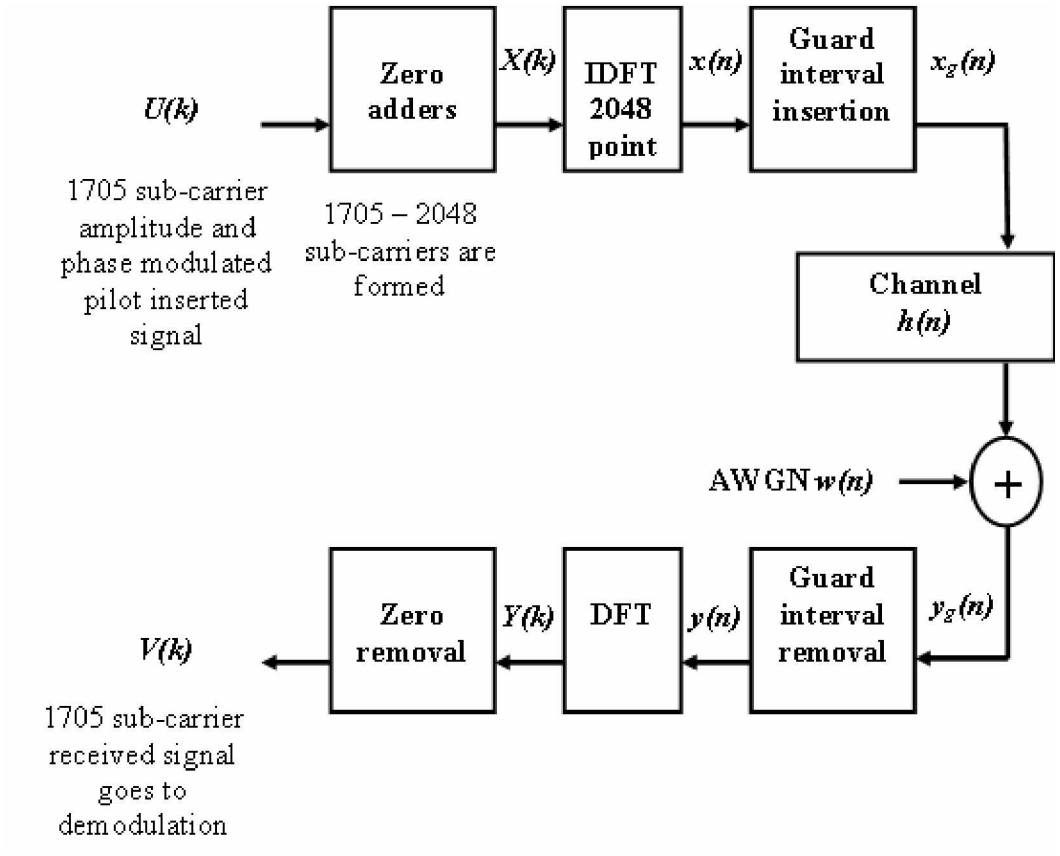

Figure 4.1: OFDM Base-band System

Binary information data are grouped and mapped into multi-amplitude, multi-phase signals as described in chapter 2. Then pilot insertion is performed. Pilot tones are inserted to sub-carriers with an order as discussed in chapter 2 and pilot locations are depicted in figure 2.7. Finally amplitude and phase modulated data is formed {U(k)}. According to DFT size which is 2048 given in standard [1] for 2K non-hierarchical mode transmission, zero padding is applied to 1705 sub-carrier data {U(k)} and we have {X(k)} with 2048 sub-carriers.

After that X(k) are sent to an IDFT and X(k) are transformed and multiplexed into {x(n)} time domain signal as

$$\begin{aligned} x(n) &= IDFT\{X(k)\} \\ &= \sum_{k=0}^{N-1} X(k) e^{j(2\pi k/N)} \quad , \\ & n = 1,2,\ldots,N-1 \end{aligned} \tag{4.1}$$

where N is the number of sub-carriers and DFT length. Then the guard interval is inserted to prevent possible inter-symbol interference (ISI) and $\{x_g(n)\}$ is formed. Guard time is chosen to be larger than the expected delay speed. This guard time includes the cyclically extended part of OFDM symbol, cyclically extended part is used to eliminate inter carrier interference (ICI) [6], [19]. The resultant OFDM symbol is given as follows;

$$x_g(n) = \begin{cases} x(N+n) & ,n=-N_g,-N_g+1,\ldots,1 \\ x(n) & ,n=0,1,\ldots,N-1 \end{cases} \tag{4.2}$$

where N_g is the length of the guard interval. The transmitted signal is then passed through the frequency selective time varying fading channel with additive Gaussian noise;

$$y_g(n) = x_g(n) \otimes h(n) + w(n) \tag{4.3}$$

, where $\otimes$ is the convolution operation, *w(n)* is Additive White Gaussian Noise AWGN and *h(n)* is the channel impulse response. The properties of *h(n)* will be described in the following chapter. At the receiver side guard interval is removed from $y_g(n)$, the received samples *y(n)* are sent to DFT block to de-multiplex the multi-carrier signal;

$$\begin{aligned} Y(k) &= DFT\{y(n)\} \\ &= \frac{1}{N}\sum_{n=0}^{N-1} y(n)e^{-j2\pi kn/N}, \\ & k = 0,1,\ldots, N-1 \end{aligned} \tag{4.4}$$

as the guard interval is chosen longer than the length of channel impulse response then there is no ISI. *Y(k)* can be expressed as;

$$\begin{aligned} Y(k) &= X(k)H(k) + W(k) + I(k) \\ & k = 0,1,\ldots, N-1 \end{aligned} \tag{4.5}$$

$$H(k) = \sum_{i=0}^{r-1} h_i e^{j\pi f_{D_i} T \frac{\sin(\pi f_{d_i} T)}{\pi f_{d_i} T} e^{-j(2\pi_i/N)k}} \tag{4.6}$$

$$\begin{aligned} I(k) = \frac{1}{N}\sum_{i=0}^{r-1}\sum_{\substack{K=0 \\ K\neq k}}^{N-1} h_i X(K) \frac{1-e^{j2\pi(f_{d_i}T-k+K)}}{1-e^{j(2\pi/N)(f_{d_i}T-k+K)}} \\ \cdot e^{-j(2\pi T_i/N)K} \end{aligned} \tag{4.7}$$

where *I(k)* is the ICI and *W(k)* is the Fourier transform of *w(n)*, assuming there is no synchronization error so *I(k)* can be omitted [17],[18].

After that, the reverse operation of zero padding is performed to *{Y(k)}* so the 1705 sub-carriers of 2048 sub-carriers *Y(k)*, *X(k)*, *H(k)*, and *W(k)* are selected and the resultant samples are *V(k)*, *U(k)*, *H'(k)*, and *W'(k)* respectively.

$$V(k) = U(k)H'(k) + W'(k) \tag{4.8}$$

It can be seen from the equation that *H'(k)* is the 1705 point part of the 2048 point channel response and *H'(k)* is multiplied with transmitted samples *{U(k)}*, so here channel effects can be modeled as a gain factor on each sample of received sample plus noise. In order to get correct transmitted samples channel effects must be cleared, to do this we follow the step given in figure 4.2.

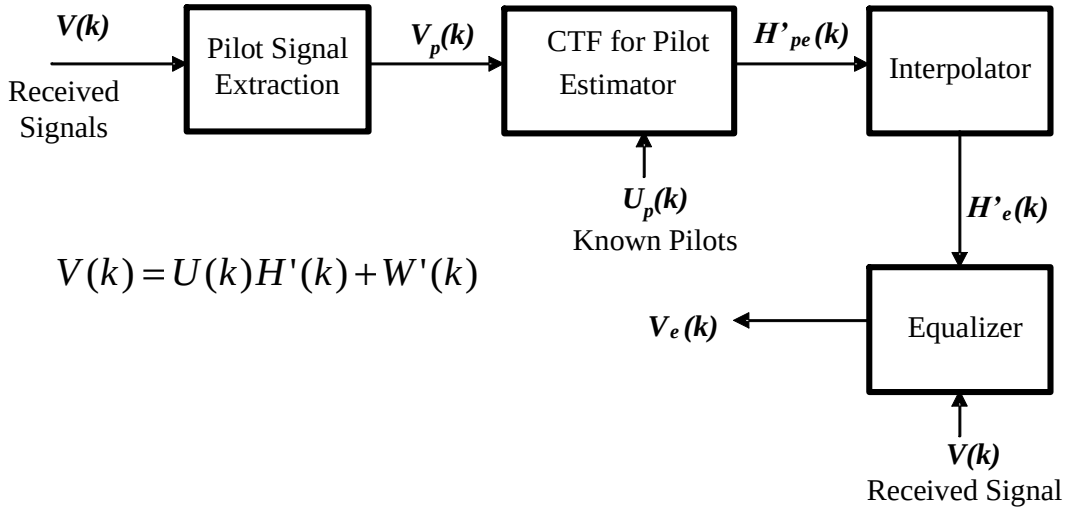

Figure 4.2: Signal Correction Model.

In DVB-T OFDM system pilot carriers are transmitted together with data carriers, so that the channel transfer function is estimated both in frequency and

time. Pilot carriers are the data symbols with an amplitude value known at the receiver [17], [20].

Then pilot signal $\{V_p(k)\}$ are extracted from $\{V(k)\}$ and the estimate of channel transfer function at pilot locations $\{H_{pe}'(k)\}$ can be obtained as receiver knows the transmitted pilot values $\{U_p(k)\}$. Finally the estimate of channel transfer function $\{H_e'(k)\}$ can be obtained by interpolating channel transfer function at pilot locations $\{H'_{pe}(k)\}$ so channel estimation is done.

With the knowledge of channel responses, the data samples $\{U(k)\}$ can be recovered using channel equalization. In the following sections channel estimation and equalization algorithms explained in detail.

4.2 Channel Estimation

The transmitted OFDM signals will be under the effect of multi-path fading, Doppler and additive noise while passing through wireless channel, which performs like a filter. In order to get correct demodulation and decoding at the receiver the channel transfer function must be estimated. For DVB-T OFDM system channel estimation is done by first estimating the channel transfer function at pilot locations and then interpolating between OFDM symbols and sub-carriers. The pilot locations are defined in DVB-T standard [1] as depicted in figure 2.3. Using equation 4.8 the received samples at pilot location can be written as

$$V_p(k) = U_p(k)H'_p(k) + W'(k) \tag{4.9}$$

where $H_p'(k)$ is the channel transfer function for pilot location. To obtain $H_p'(k)$ beforehand DFT of Gaussian noise $\{W'(k)\}$ has to be known.

$$\frac{V_p(k) - W'(k)}{U_p(k)} = H'_p(k) \tag{4.10}$$

Let the estimation of channel transfer function at pilot locations to obtain transmitted pilots signal correctly, be $H_{pe}'(k)$ so

$$\frac{V_p(k)}{U_p(k)} = H'_{pe}(k) \tag{4.11}$$

As it is difficult to obtain exact $W'(k)$, accurate estimation of channel transfer function at pilot locations $\{H_{pe}'(k)\}$ is necessary. In the following sections four Types of channel estimation are investigated, least square (LS) estimation, linear minimum mean square error (LMMSE) estimation with known channel transfer function, linear minimum mean square error (LMMSE) estimation with utilizing the result of LS estimation result and minimum mean square error (MMSE) estimation with the assumption of noise to be white and its variance is known.

4.2.1 Least Square (LS) Estimation

The least square estimator is the simple estimator that can be implemented. The basic principle is dividing the received samples by the actually transmitted samples, with the assumption of transmitted samples are known [17], [18], [21], [22]. In estimating channel transfer function at pilot case, transmitted pilot samples have already known at the receiver so the LS estimator is written as:

$$H'_{peLS}(k) = \frac{V_p(k)}{U_p(k)} \tag{4.12}$$

The division operation used in LS estimator is element-wise division. Although it is a simple model with only one division per carrier, the effect of noise cannot be mitigated and if some values of $V_p(k)$ is zero at pilot location estimation of channel transfer function involved zeros , since LS estimator is susceptible to additive noise MMSE is proposed but MMSE includes matrix inversion at each iteration, so the simplified MMSE estimator given in [23], [24], [25] is suggested.

4.2.2 Linear Minimum Mean Square Estimation

This estimator minimizes the mean square error between the actual and estimated channels. The name of the linear estimation is come from applying a linear transformation to LS estimate $\{H'_{peLS}\}$. The LMMSE estimator has been shown to be better than LS estimate for channel estimation in OFDM systems [26]. The LMMSE estimate of the channel transfer function at pilot $\{H'_{peLMMSE}\}$ *is* given in [17], [23], and [26]

$$\begin{aligned} R_{HH} &= R_{H'_p H'_p} = E\{H'_p H'^{H}_p\} \\ H'_{peLMMSE} &= R_{HH}(R_{HH} + \sigma_n^2 (U_p U_p^H)^{-1})^{-1} H'_{peLS} \end{aligned} \tag{4.13}$$

where σ_n^2 is the variance of additive noise, R_{HH} is the channel auto-correlation matrix uses real channel transfer function for pilot locations. The superscript $(.)^H$ is the conjugating transpose which is called Hermitian transpose. Note that there is a matrix inverse involved in the estimator which must be

calculated every time when U_p is changed. This problem can be solved using the statistics of pilots.

After that LMMSE is reduced to:

$$\beta = E\{|U_p|^2\}E\{|1/U_p|^2\}$$
$$H'_{peLMMSE} = R_{HH}(R_{HH} + \beta / SNR)^{-1} H'_{peLS} \quad (4.14)$$

where β is a constant depending on signal constellation. In the case of DVB-T OFDM pilots are mapped using Differential Binary Phase Shift Keying (DBPSK) so β =1.

In this estimation R_{HH} and SNR are used so variance of noise and channel response have to be known beforehand or can be calculated accurately in the receiver. In our performance analysis we use the LS estimate $\{H'_{peLS}\}$ to calculate R_{HH} the performance results are given in the end of the chapter and still The LMMSE estimator has been shown to be better than LS estimator. The major drawback of LMMSE estimate is its high complexity, which grows exponentially with the observation samples.

4.2.3 Minimum Mean Square Estimation

In [27], [28] an MMSE approach is proposed for channel equalization, we use this approach to estimate the channel.

The MMSE equalizer given in [27] is:

$$U_{pe}(k) = \frac{[H'_p(k)]^* \bullet V_p(k)}{H'_p(k) \bullet [H'_p(k)]^* + 1/SNR} \quad (4.15)$$

Where • is the element wise multiplication operation. As in the LMMSE approach still SNR and real channel transfer function have to be known. For estimating the channel we redefine formula as

$$H'_{peMMSE}(k) = \frac{[V_p(k)]^* \bullet U_p(k)}{V_p(k) \bullet [V_p(k)]^* + 1/SNR} \qquad (4.16)$$

The estimation performances of all there algorithms are given in the end of the chapter. Assuming the noise is white and noise variance σ_n^2 and variance of $U_p(k)$ σ_u^2 is known so SNR= σ_n^2/σ_u^2.

4.2.4 Interpolation Methods

After the channel estimation of the channel transfer functions of pilot tones, the channel responses of data tones can be interpolated according to adjacent pilot tones. In DVB-T OFDM pilots are scattered uniformly in OFDM symbols as depicted in figure 2.7 so interpolations in both time and frequency direction is possible.

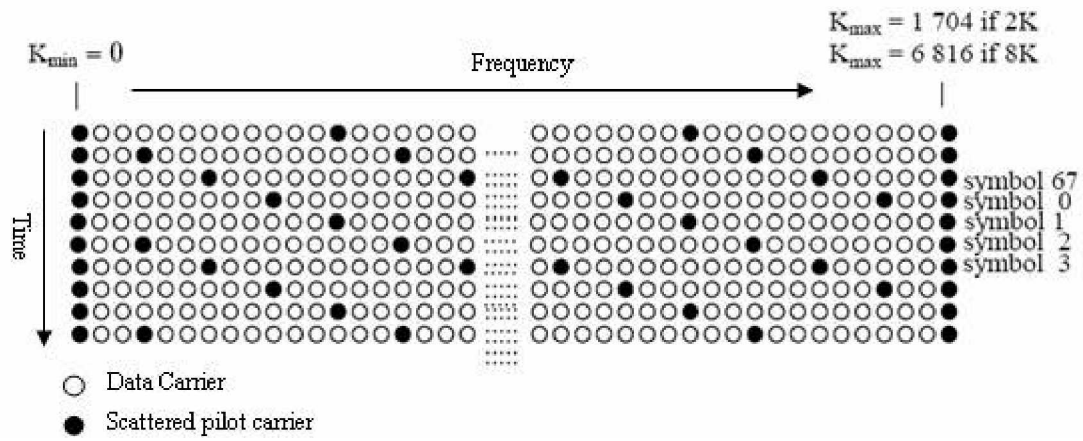

Figure 4.3: Pilot and data carriers pattern for DVB-T 2k and 8k modes.

Figure 4.2 shows the scattering pattern of pilot carriers for OFDM symbols for 2k and 8k modes. For 2k mode there are $S_{2k}=I43$ scattered pilot carriers with a distance $l_f=12$ in frequency direction so they became with a distance of l_t=4 in time direction [20]. According to scattered pattern to assure correct channel estimation time interpolation has to be performed first. After time interpolation the pilot spacing in frequency direction becomes $l_f=3$. So in DVB-T system 3 data carriers in time direction interpolates after that 2 data carriers are interpolated in frequency direction. In order to evaluate performance of interpolation algorithms the pilot configuration is crucial. For the considered DVB-T system $H'_{pe}(k)$ is the channel transfer function at pilot location and $H'_e(k)$ is the interpolator output. According to sampling theorem, it is possible to exactly reconstruct a band-limited function if the sample interval t_s is smaller than $1/f_m$ where f_m is the frequency limit of the function but to obtained this ideal filter must be used. $H'_e(k)$ is a band limited function in both time and frequency direction because it is basically the frequency response of the channel. Channel transfer function's (CTF) real and imaginary values in frequency direction for Raleigh multi-path fading channel used in this thesis is depicted in figure 4.4 and 4.5 respectively, and the frequency response of this function is depicted in figure 4.6.

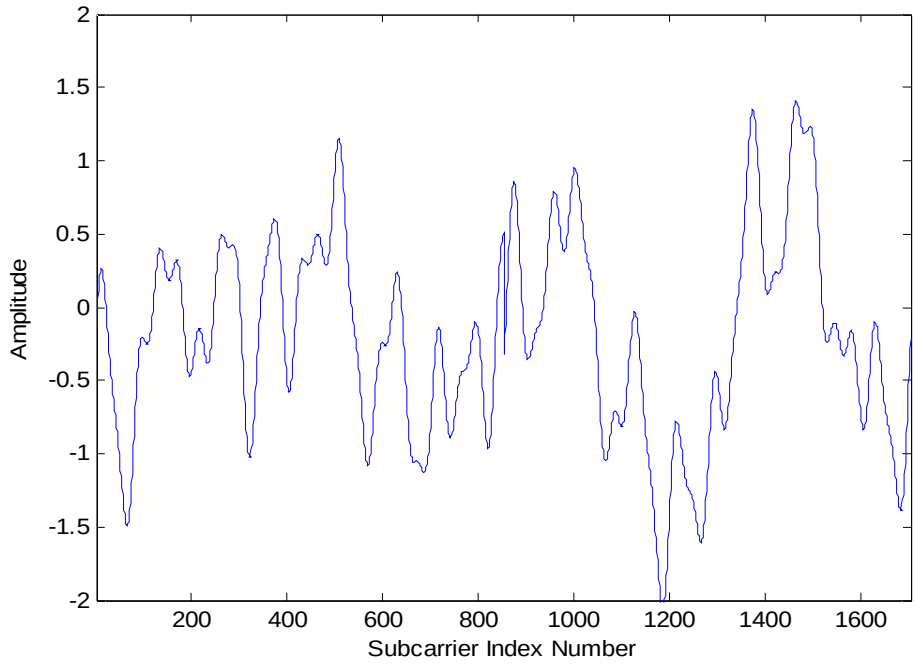

Figure 4.4: Real values of channel transfer function for the Raleigh multi-path fading channel.

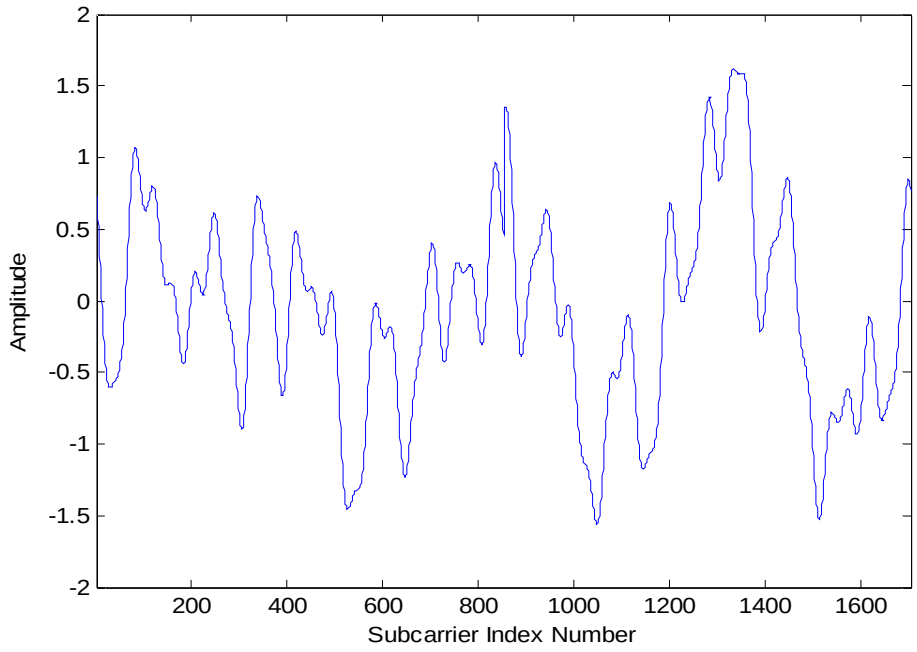

Figure 4.5: Imaginary values of channel transfer function for the Raleigh multi-path fading channel.

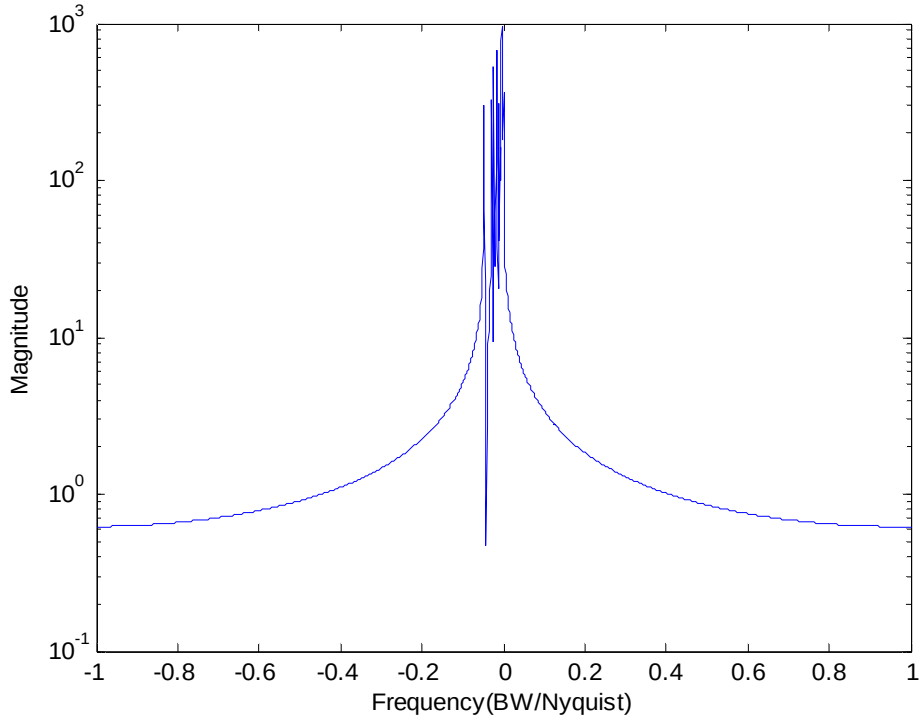

Figure 4.6: Frequency response of channel transfer function.

The CTF values are given for noiseless channel case and as the band-with of CTF is very narrow it may be considered that CTF is over-sampled. If the values at data locations are omitted from this CTF it becomes that the time interpolated version of $H'_{pe(k)}$. In the following figure the frequency response of the channel transfer function for the pilot carriers in frequency direction with nulls at data locations is depicted.

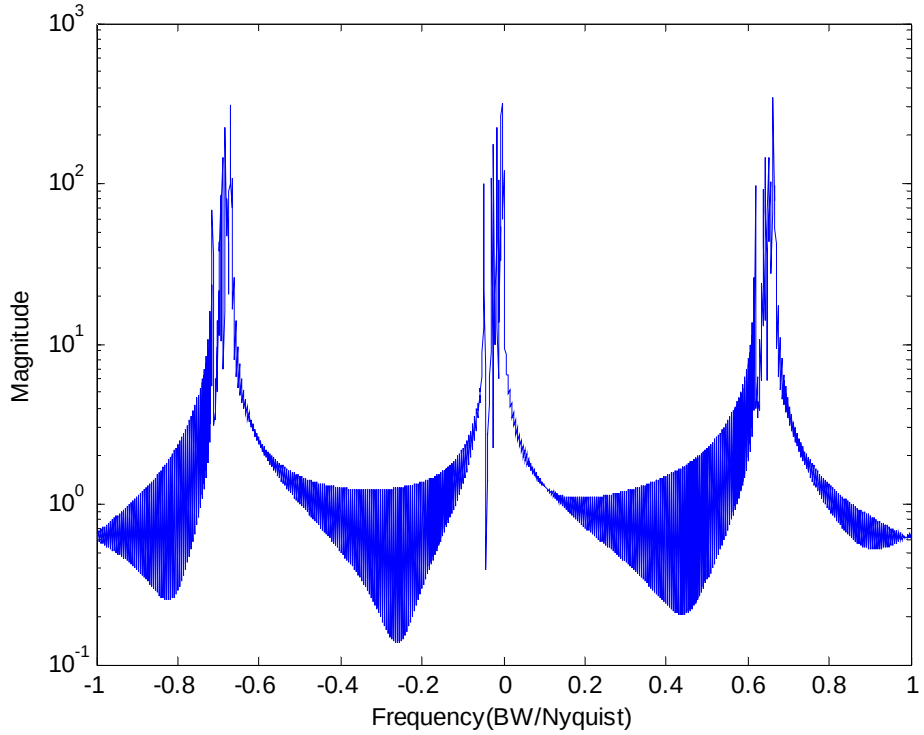

Figure 4.7: Frequency response of time interpolated channel transfer function at pilot locations with nulls at data locations in frequency direction.

In figure 4.6 it can be seen the exact part of the CTF function and its frequency-scaled images. To obtain the required CTF from time interpolated pilots given in figure 4.6 an ideal low pass filter must be used. This operation can be considered as increasing the sample rate of time interpolated $H'_{pe(k)}$ in frequency direction. The ideal filter can be named as ideal low-pass interpolation filter. In practical case, ideal low-pass interpolation filter cannot be implemented exactly, but very good approximations can be designed [29].

Although ideal interpolation gives the best result, other interpolation techniques may be efficient for DVB-T case.

In this thesis several interpolation methods which are linear, low-pass, spline, and DFT [18], [20], [29], [30], [31], [32] are investigated. For time interpolation three approaches for frequency interpolation four approaches are used.

4.2.4.1.1 Low-pass Interpolation

The low-pass interpolation is simply performed by inserting zeros to original sequence and then filtering this sequence using a low-pass FIR filter. In [33] *interp* function in MATLAB is used for low-pass interpolation. *Interp* function designs a special symmetric FIR filter that allows the original data to pass through unchanged and interpolates between so that the mean-square errors between the interpolated points and their ideal values are minimized, it uses the special low-pass interpolation in [34].

As a second low-pass filter a Parks-McClellan optimal FIR equiripple low-pass filter is used based on MATLAB function *firpm*. The Parks-McClellan algorithm designs filters using the *firpm* exchange algorithm and Chebyshev approximation theory with an optimal fit between the desired and actual frequency responses. Parks-McClellan algorithm optimizes the filter that the maximum error between the desired frequency response and the actual frequency response is minimized finally filters have an equiripple behavior in their frequency responses and are sometimes called equiripple filters. *firpm* exhibits discontinuities at the head and tail of its impulse response due to this equiripple nature [35].

4.2.4.1.2 Linear Interpolation

In the linear interpolation algorithm, two successive pilot sub carriers are used to determine the channel response for data sub-carriers that are located in between the pilots; it is often the best solution for time interpolation, since it only requires 2 points to be known. It can be performed by convolution of the

extracted channel transfer function at pilot locations with a triangular impulse function shown in figure 4.8. [20]

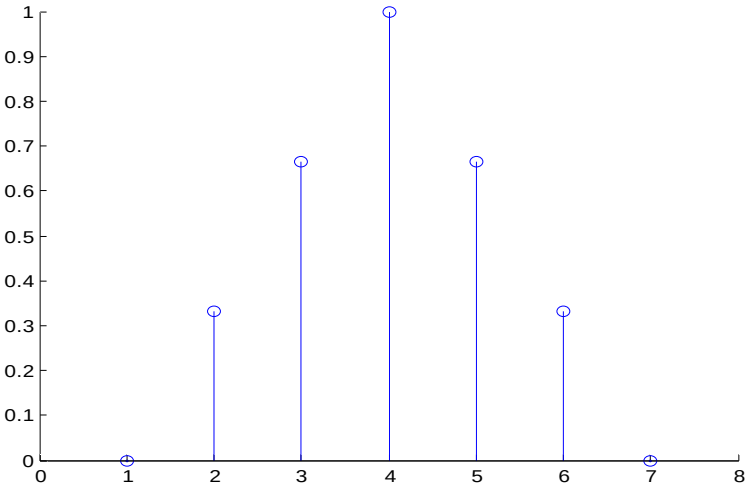

Figure 4.8: Linear interpolation filter.

This filter can fill 2 null samples between pilots. Linear interpolation can be implemented by simple methods [17], [18], [21], [32].

In the frequency response although linear interpolation filter has a wide pass band and transition regions it can perform accurately for DVB-T pilot configuration. The frequency response of the linear interpolation filter, time interpolated CTF at pilot locations with nulls at data locations in frequency direction, and Parks-McClellan optimal FIR equiripple low-pass filter shown in figure 4.9.

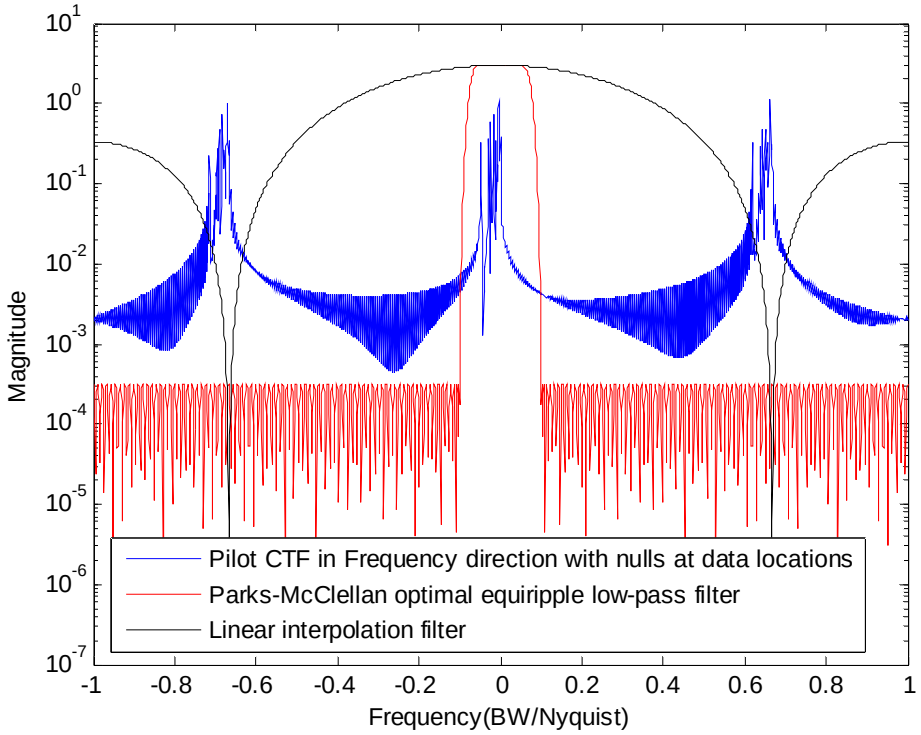

Figure 4.9: Illustration of linear and low-pass interpolation in frequency direction.

From the figure we see that the original sampling rate is much higher than Nyquist rate so linear interpolator has a flat response in the desired window and the response of linear interpolator has small values at the frequency scaled images of CTF so linear interpolator in DVB-T has better performances. This is reasonable because original sampling rate greatly exceeds the Nyquist rate so the signal will not vary significantly between samples, thus linear interpolation should be more accurate for over-sampled signal [38] and the implementation of linear interpolation is simple and also requires smaller time and memory than the other interpolation types In channel estimated for noisy channels linear interpolation filter has poor performances compared with low-pass interpolation because it is not filter noise as good as low-pass filters. Performances of this interpolation algorithms are compared in the following sections.

4.2.4.1.3 Spline Interpolation

Spline interpolation produces a smooth and continuous polynomial fitted to given data points. The real components of the known sub-carriers are taken and a special curve [32] is fitted between them imaginary components are pass through from same idea then real and imaginary components are combined to for a final frequency domain estimate is for all sub-carriers. Its implementation is not very complicated because it requires minimum of three known pilots.

4.2.4.1.4 DFT Interpolation

After time interpolation using one of the linear, interpolator or low-pass interpolator DFT based interpolation can be used for frequency interpolation [30]. Time interpolated $H'_{pe}(k)$ can be named as $H't_{pe}(k)$**.** Basically DFT interpolation performed by first transforming $H't_{pe}(k)$ to time domain using IDFT after that to obtain required sub-carrier size zero inserted to time domain data and $G_{pe}(k)$=[$IDFT(H't_{pe}(k))$ 0 0 0 ...] is formed than the time domain profile is transform back to frequency domain using DFT which becames $H'_e(k)=DFT(G_{pe}(k)))$. Although DFT interpolation approach is a good interpolation method in our case it is not because the efficient implementation of the DFT-based approach employing FFTs restricted to pilot number to be a power of 2.[22] In DVB-T 2k mode after time interpolation this value becomes 569.

4.3 Channel Equalization

After estimating the channel, the received signal needs to be equalized. If the cyclic prefix is longer than the maximum delay spread of the channel, we can model the effect of channel as a complex multiplication in frequency domain as described in chapter 3.

For channel equalization two methods is used which described in [27] which are zero forcing (ZF) and minimum mean-square error(MMSE). We use the abbreviation MMSE4 for MMSE in [27] in this thesis. The two equalizer are:

ZF equalizer:

$$U_e(k) = \frac{V(k)}{H'_e(k)} \tag{4.17}$$

MMSE4 equalizer:

$$U_e(k) = \frac{[H'_e(k)]^H \bullet V(k)}{H'_e(k) \bullet [H'(k)]^H + 1/SNR} \tag{4.18}$$

Where • is the element wise multiplication operation and $(.)^H$ is the hermitian transpose. Assuming the noise is white and noise variance σ_n^2 and variance of $U(k)$ σ_u^2 is known so SNR= σ_n^2/σ_u^2.

Using MMSE4 minimizes the influence of AWGN on the equalization. Noise adds uncertainty to the magnitudes and phase of data samples in OFDM symbol. During equalization noise effects are increased. Using MMSE4 this effect nearly compensated. Performance analysis of this two channel equalization types are evaluated in the next following sections.

4.4 Performance Analysis

In this section we compare all the algorithms and methods investigated about channel estimation, channel equalization and interpolation algorithms. We assume to have perfect synchronization since we want to compare channel estimation, channel equalization and interpolation algorithms. We have chosen

guard interval to be grater than the maximum delay spread in order to avoid inter-symbol interferences. Simulations are takes place in MATLAB release 14.

Performance results are given in the name of Coded BER, Un-coded BER and Channel MSE which are the Viterbi decoder output BER performances, OFDM demodulator output BER performances and channel mean-square error performances respectively. DVB-T OFDM system parameters are given below.

Table 4.1: DVB-T OFDM system parameters

PARAMETERS	**SPECIFICATIONS**
FFT size	2048
Number of carriers	1705
Number of pilots in frequency Direction	143
Guard interval size	512
Baseband Signal Modulation	16QAM
Pilot Modulation	DBPSK
Punctured Code Rate	3/4
Demodulation Resolution	8 bit
Carrier Spacing	4464 Hz
Symbol duration	224 μs
Symbol duration with Guard Time	280 μs
Bandwith	7.61 MHz
Coding Parameters	Described in Chapter 2
Channel	Rayleigh, Rician Fading with Doppler effect
Simulation step	500

4.4.1.1.1 Performance Analysis of Channel Estimation

Four different types of channel transfer function for pilot location estimation is performed these are Least square (LS) estimation, linear minimum mean-square error estimation using least square channel transfer function values (LMMSE with LS), linear minimum mean-square estimation using real channel transfer function (LMMSE) and minimum mean square error estimation. For LMMSE the noise variance and channel transfer function assumed to be known also in MMSE variance of noise and variance of transmitted symbols assumed to be known.

In the following figures the channel estimation performances are compared in the sense of channel transfer functions mean-square errors (channel (CTF) MSE) for different types of interpolation algorithms under Rayleigh multipath fading channel.

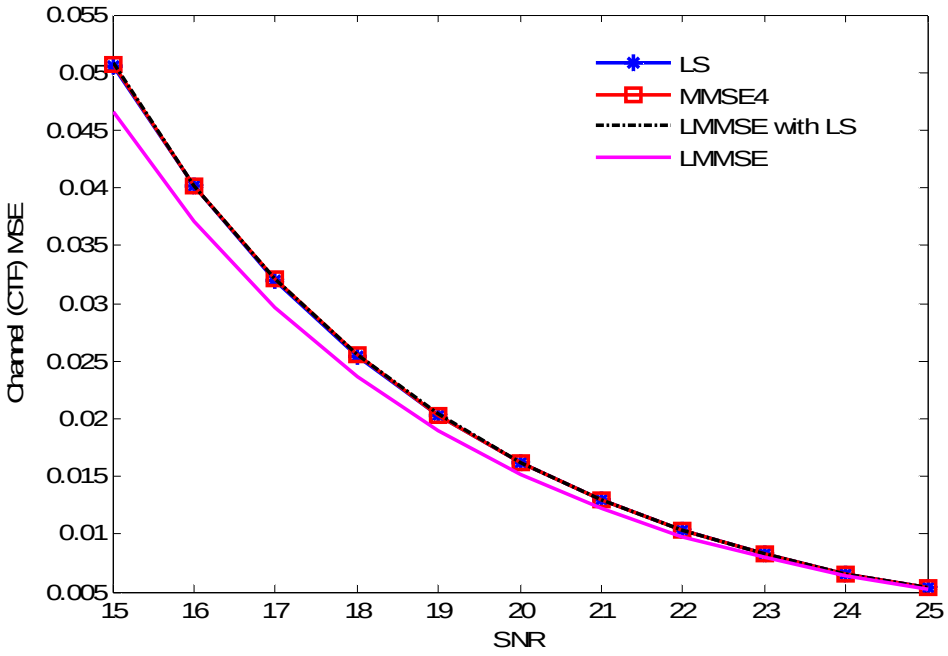

Figure 4.10: The MSE of Channel transfer functions for different channel estimations. Linear Time and Linear Frequency interpolation is used under Rayleigh fading channel.

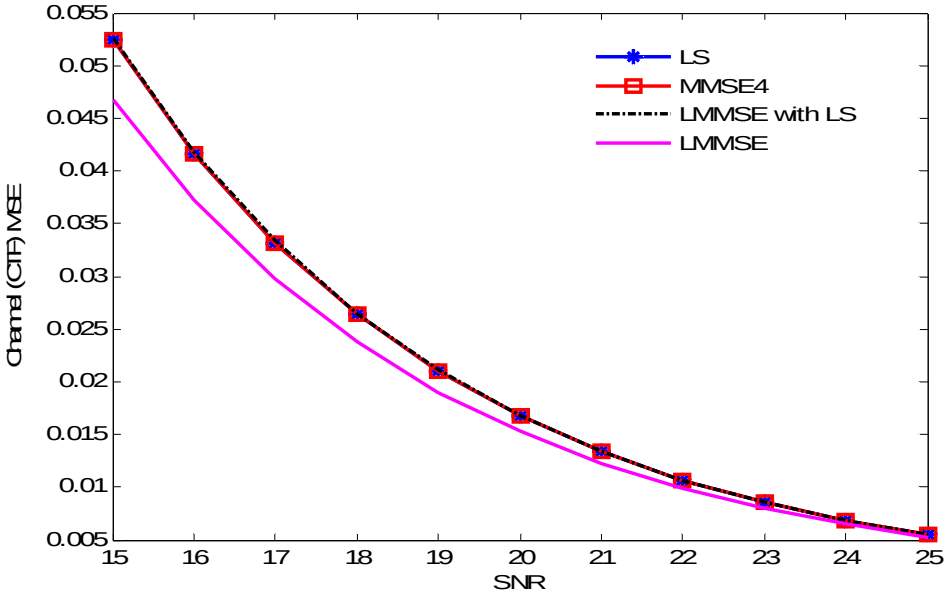

Figure 4.11: The MSE of Channel transfer functions for different channel estimations. Linear Time and Spline Frequency interpolation is used under Rayleigh fading channel.

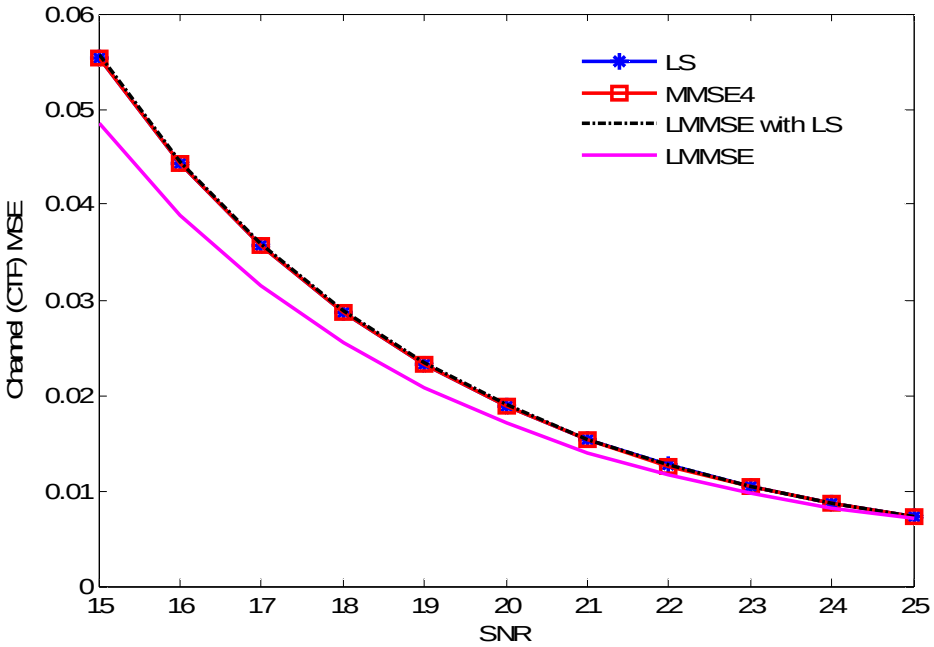

Figure 4.12: The MSE of Channel transfer functions for different channel estimations. Linear Time and DFT Frequency interpolation is used under Rayleigh fading channel.

The preceding figures show the comparisons between channel estimation algorithms for linear time interpolation and linear, spline and DFT frequency interpolation under Rayleigh multipath fading channel. It is obtained that for the given channel estimation algorithms LMMSE has slightly better performances according to other three types. The differences vanish for higher SNR, but increases for lower SNR this is expected because LMMSE estimation is proposed to mitigate noise effects in CTF.

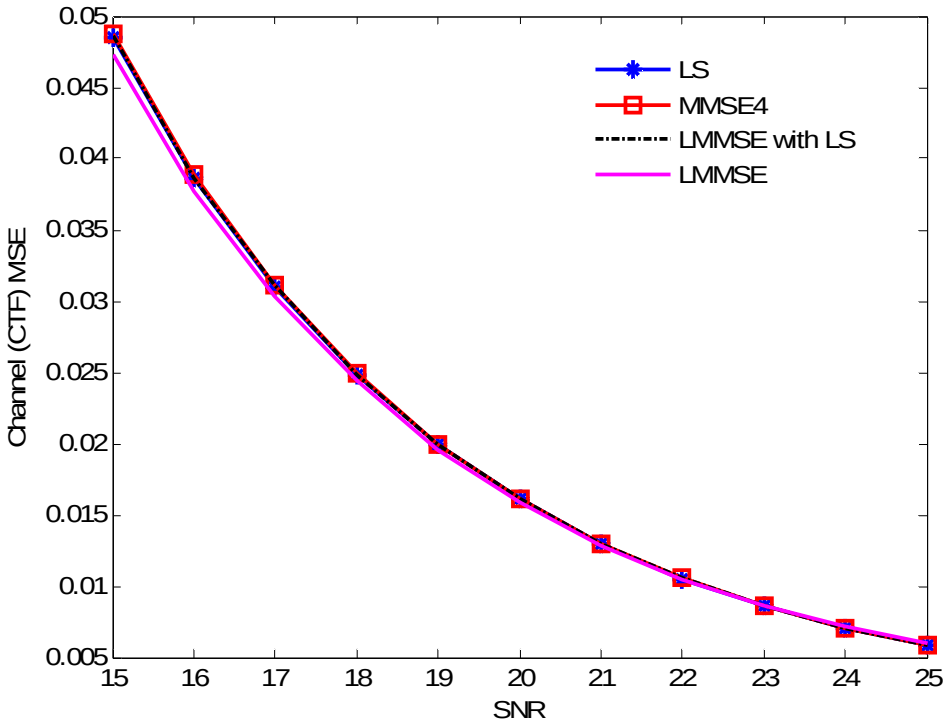

Figure 4.13: The MSE of Channel transfer functions for different channel estimations. Linear Time and Low-pass Frequency interpolation is used under Raleigh fading channel.

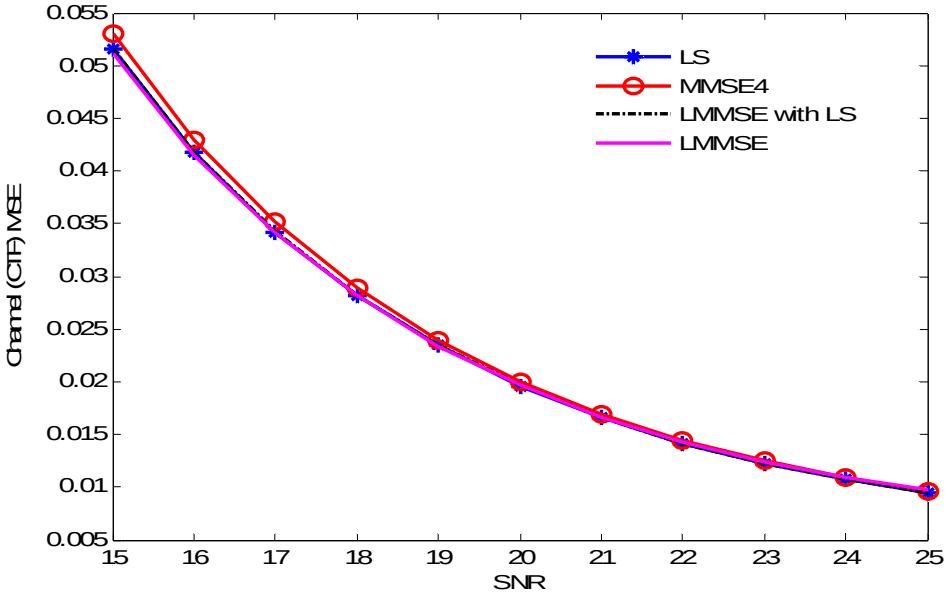

Figure 4.14: The MSE of Channel transfer functions for different channel estimations. Low-pass with a narrow pass-band Time and Low-pass Frequency interpolation is used under Raleigh fading channel.

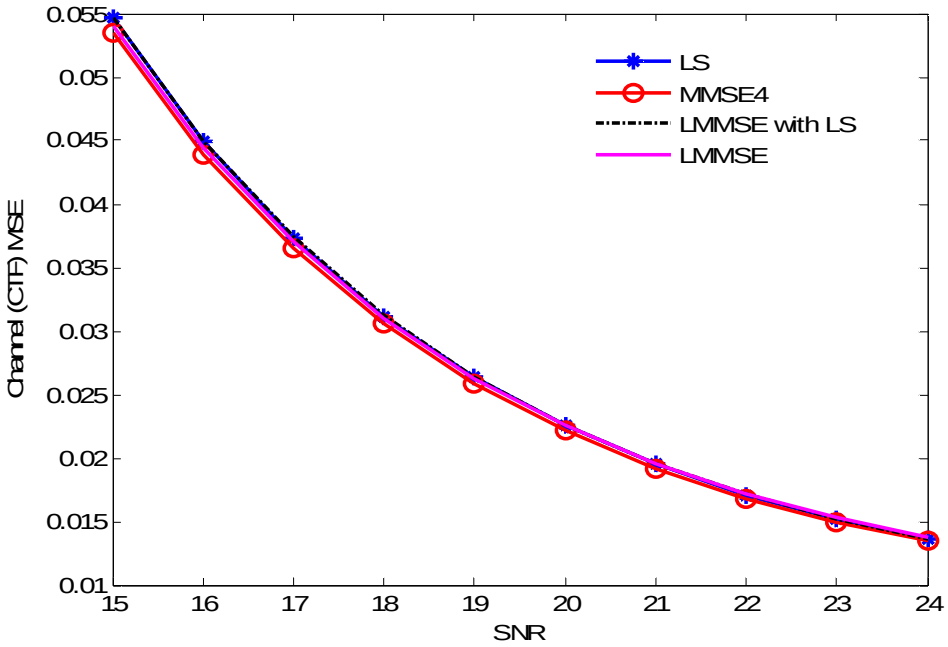

Figure 4.15: The MSE of Channel transfer functions for different channel estimations. Low-pass with a wide pass-band time interpolation and low-pass frequency interpolation is used under Rayleigh fading channel.

The preceding figures show the comparisons between channel estimation algorithms for linear time, low-pass frequency interpolation, low-pass time, low-pass with a narrow band low-pass frequency interpolation and low-pass with a wide band low-pass frequency interpolation under Rayleigh multipath fading channel. The comparisons are in the means of MSE. It is obtained that the four given channel estimation algorithms has nearly same performances. This can be explained using the fact that low-pass interpolation filters noise. The efficiency of LMMSE comes in the means of noise mitigation but also noise can be filtered by low-pass interpolation so other three channel estimation algorithms achieved similar performances with LMMSE in the means of MSE.

Next figure gives performance results for the same methods but in this figures 100 Hz of Doppler Effect added to transmitted data under Rayleign multipath fading channel.

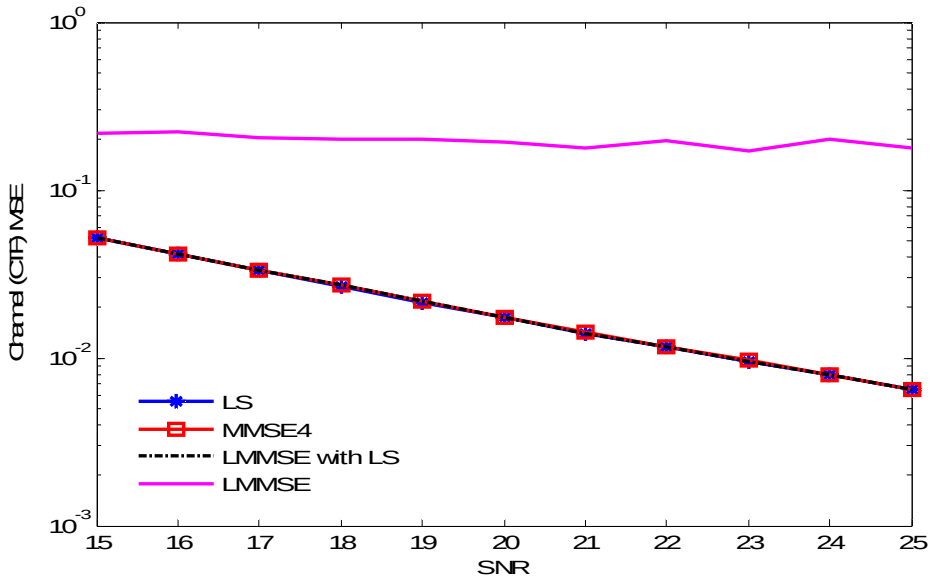

Figure 4.16: The MSE of Channel transfers function for channel estimations. Linear Time and Linear Frequency interpolation is used under Raleigh fading channel with 100Hz Doppler Shift

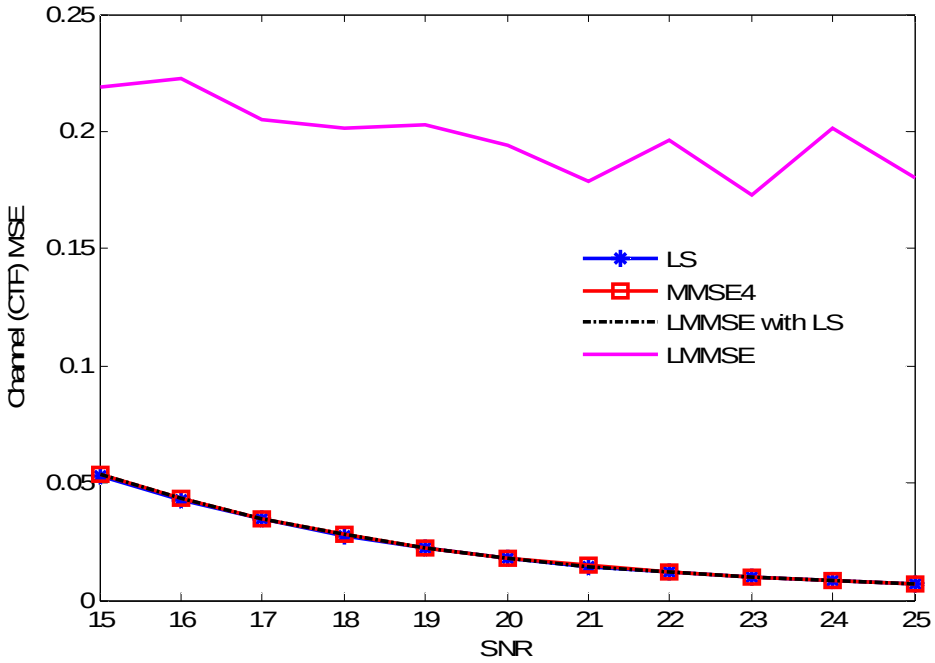

Figure 4.17: The MSE of Channel transfers function for channel estimations. Linear Time and Spline Frequency interpolation is used under Raleigh fading channel with 100Hz Doppler Shift.

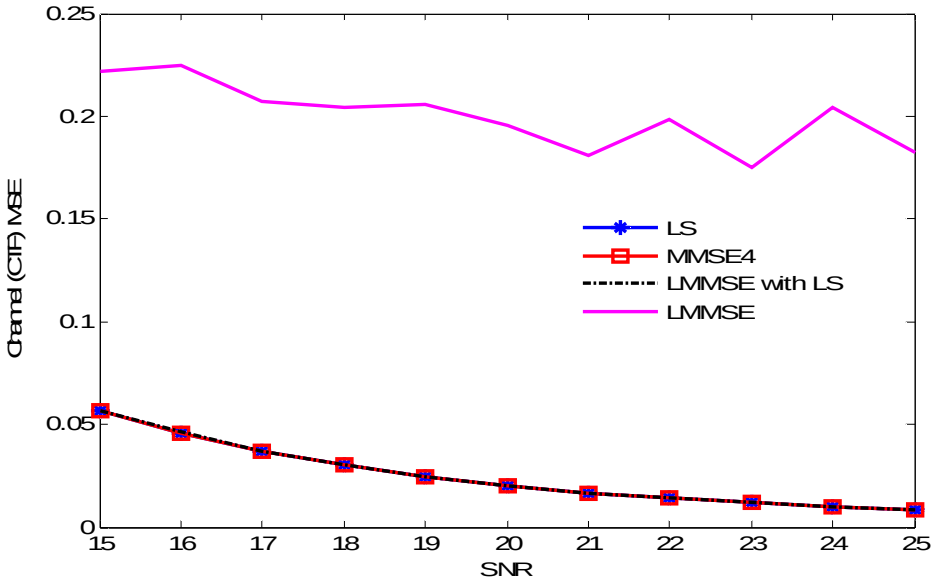

Figure 4.18: The MSE of Channel transfers function for channel estimations. Linear time and DFT frequency interpolation is used under Raleigh fading channel with 100Hz Doppler Shift.

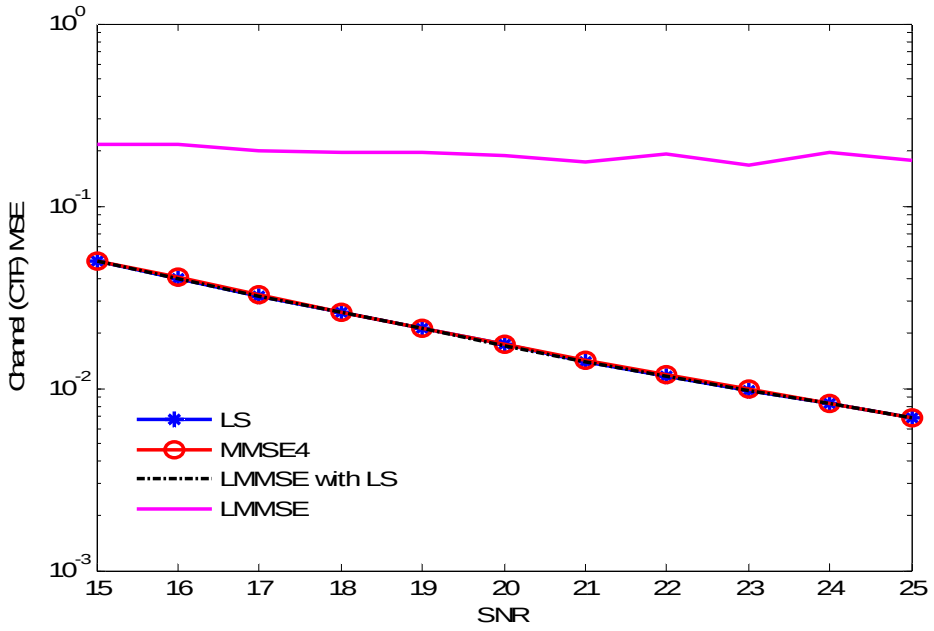

Figure 4.19: The MSE of Channel transfers function for channel estimations. Linear Time and Low-pass Frequency interpolation is used under Raleigh fading channel with 100Hz Doppler Shift.

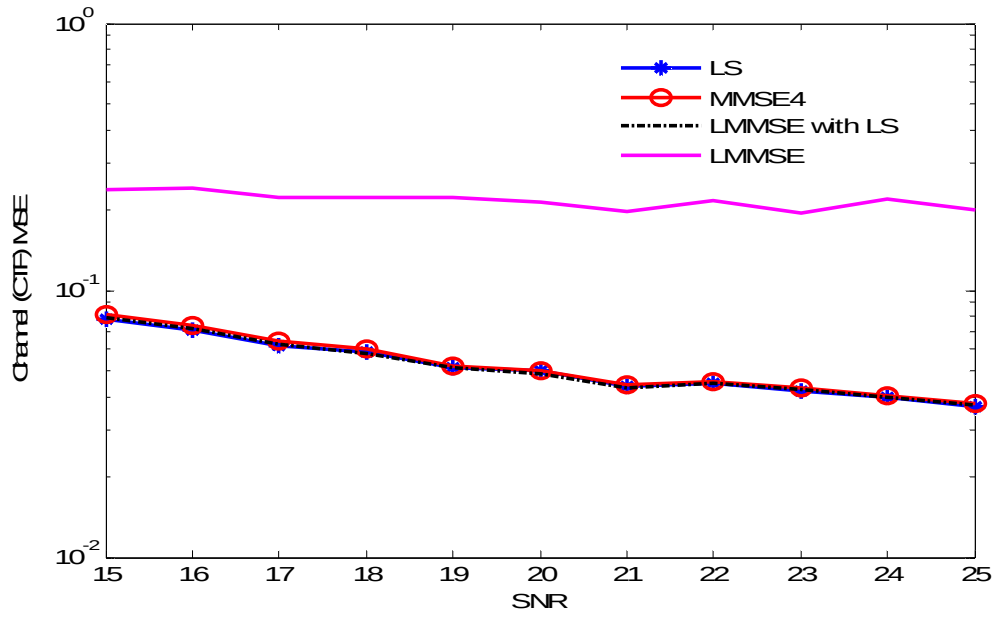

Figure 4.20: The MSE of Channel transfers function for channel estimations. Low-pass with a narrow pass-band Time and Low-pass Frequency interpolation is used under Raleigh fading channel with 100Hz Doppler Shift

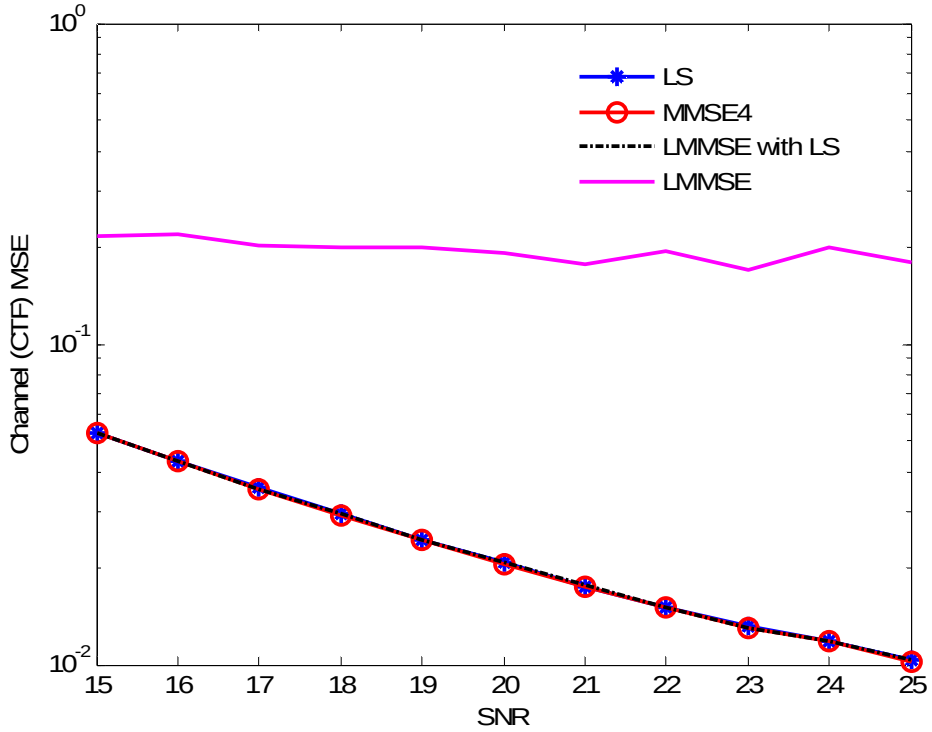

Figure 4.21: The MSE of Channel transfers function for channel estimations. Low-pass with a wide pass-band Time and Low-pass Frequency interpolation is used under Raleigh fading channel with 100Hz Doppler Shift

These figures show the comparisons between channel estimation algorithms for all implemented interpolation algorithms under Rayleigh multipath fading channel with Doppler Effect of max 100Hz. The comparisons are in the means of MSE. It is obtained that the three given interpolation algorithms has nearly same performances. Although LMMSE has the best performances for no Doppler Effect case here it is the worst one. According to equation 4.13 correlation matrix is calculated using real channel transfer function so in Doppler Effect case this function cannot be assumed it depends on the Doppler Frequency value.

Based on these results for no Doppler effect case LMMSE has the best performance in the means of MSE, other three channel estimation algorithms have nearly the same performances for all the interpolation algorithms. As LS, LMMSE with LS and MMSE4 has nearly same performances LS estimation is

chosen for the optimum channel estimation case because it is the simple algorithm in the means of implementation.

After that for a max 100Hz Doppler effect case the best channel estimation methods becomes LS, LS with LMMSE and MMSE4 so again LS can be chosen for optimum and best case. After deciding the channel estimation algorithms for different channel effects, the optimum interpolation algorithm or algorithms needed to be determined. In the next section we compare interpolation algorithms.

4.4.1.1.2 Performance Analysis of Interpolation Algorithms

Performance analysis of 2D interpolation algorithms are evalueted. Six types of combinations are simulated for the optimized channel estimation algorithms and for the two types of equalization algorithms. Six types of interpolation algorithms are linear time interpolation to linear, spline, DFT, low-pass frequency interpolations, a narrow-band low-pass time interpolation to a low-pass frequency interpolation and wide-band low-pass time interpolation to low-pass frequency interpolation. Performance results are compared according to the BER of Viterbi decoded data under Rayleigh fading channel for both 100Hz Doppler Effect case and no Doppler Effect case.

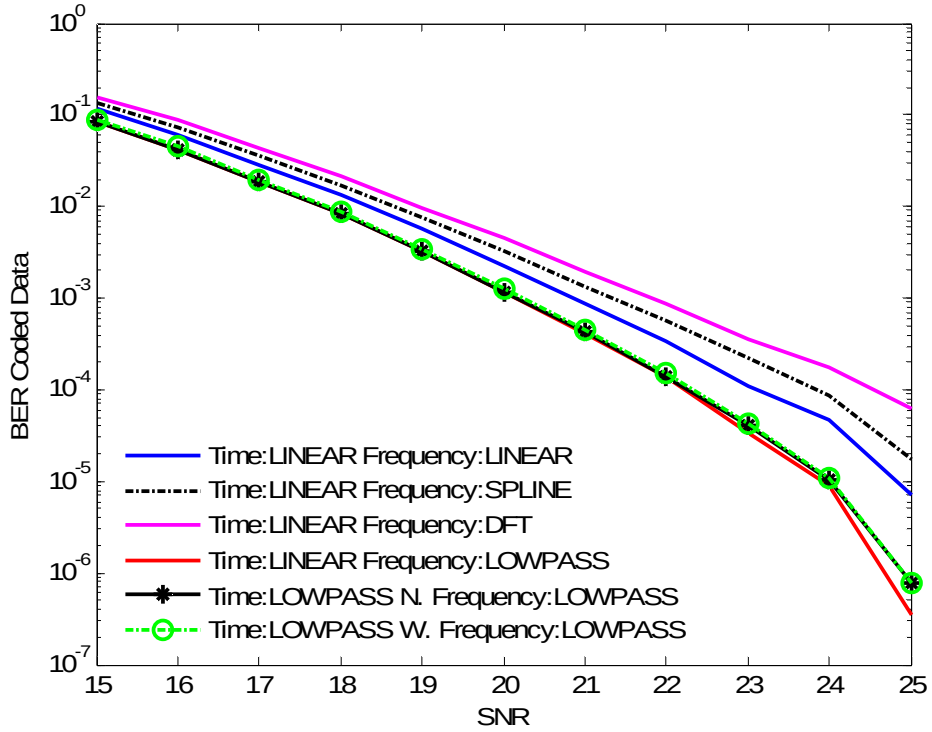

Figure 4.22: BER of data after Viterbi decoder for different interpolation algorithms. LS channel estimation and ZF channel equalization is used under Raleigh fading channel.

In Figure 4.22 coded BER performances are given for six types of interpolation algorithms for LS channel estimation and ZF channel equalization under Rayleigh fading channel. It is clear that the DFT and Spline interpolation is the worse than the other interpolation. The performances of low pass interpolator at the frequency direction gives similar to each other and good results according to other interpolations. LS channel estimation and ZF equalization is vulnerable to noise effects so low pass interpolators performance values are better than others because they can compensate noise effects better than others.

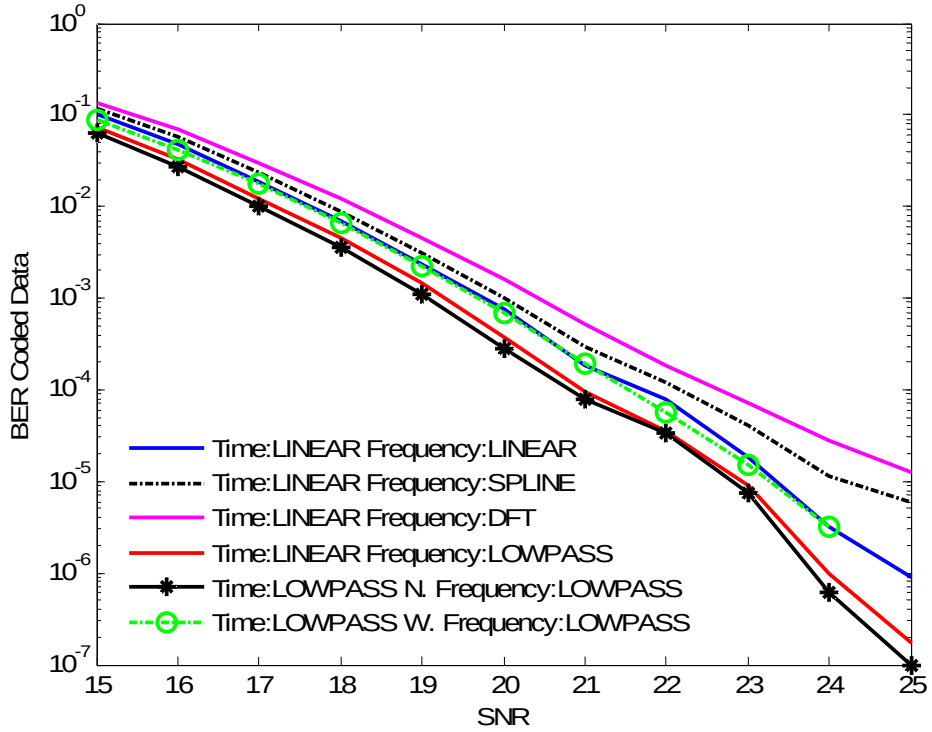

Figure 4.23: The BER of data after the Viterbi decoder for different interpolation algorithms. LS channel estimation and MMSE4 channel equalization is used under Raleigh fading channel.

In Figure 4.23 coded BER performances are given for six types of interpolation algorithms for LS channel estimation and MMSE4 channel equalization under Rayleigh fading channel. However MMSE4 mitigate the effects of noise low-pass with narrow band interpolator has the best performance because the pass band of this interpolator is very narrow so as the response of channel transfer function is seems to be over-sampled all the desired response includes the proposed filters pass band regions also linear time and low-pass frequency has good approximation to narrow-band low-pass filter. The performances of DFT and Spline cubic are not good interpolators under this case.

Table 4.2: Required SNR for different interpolation algorithms and for different channel equalization methods to achieve BER=$2x10^{-4}$ after the Viterbi decoder. LS channel estimation is used under Raleigh fading channel.

Required SNR(dB) for BER=$2x10^{-4}$ after Viterbi, QEF after Reed-Solomon	**Channel Estimation/ Equalization Method**	
Interpolation Algorithm Time/Frequency	LS/ZF	LS/MMSE4
Linear Time/Linear Frequency	*22.47*	*20.94*
Linear Time/Spline Frequency	*23.11*	*21.44*
Linear Time/DFT Frequency	*23.80*	*21.93*
Linear Time/Low-pass Frequency	*21.66*	*20.46*
Narrow Band Low-pass Time/ Low-pass Frequency	*21.69*	*20.27*
Wide Band Low-pass Time / Low-pass Frequency	*21.76*	*20.99*

Table 4.3: Required SNR for different interpolation algorithms and for different channel equalization methods to achieve BER=$2x10^{-4}$ after the Viterbi decoder. LMMSE channel estimation is used under Raleigh fading channel. shows the required SNR results for QEF communication in the output of Reed-Solomon (RS) Decoder which is a BER of $2x10^{-4}$ at the Viterbi decoder output. For the same interpolation algorithms MMSE4 equalization has clearly better performances. The better approach for interpolation is low-pass, but linear time, linear frequency interpolation algorithms can also be considered because of simple implementation and minimizing storage memory.

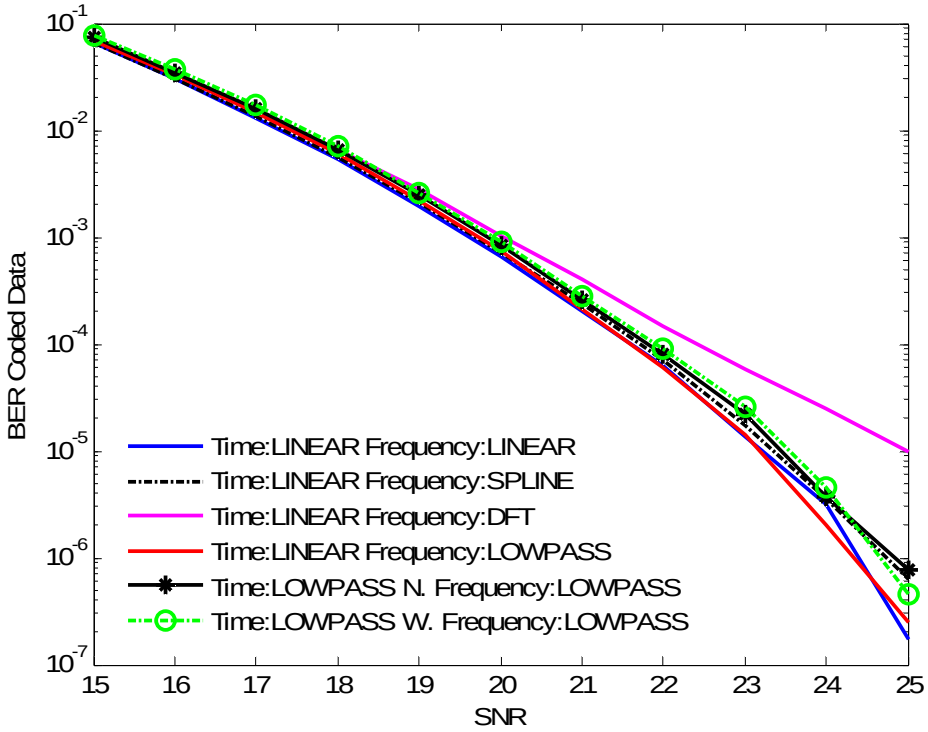

Figure 4.24: BER of data after Viterbi decoder for different interpolation algorithms. LMMSE channel estimation and ZF channel equalization is used under Raleigh fading channel.

In Figure 4.24 coded BER performances are given for six types of interpolation algorithms for LMMSE channel estimation and ZF channel equalization under Rayleigh fading channel. As LMMSE mitigate the effects of noise linear and spline interpolations becomes better and achieved to the performances of low-pass interpolators.

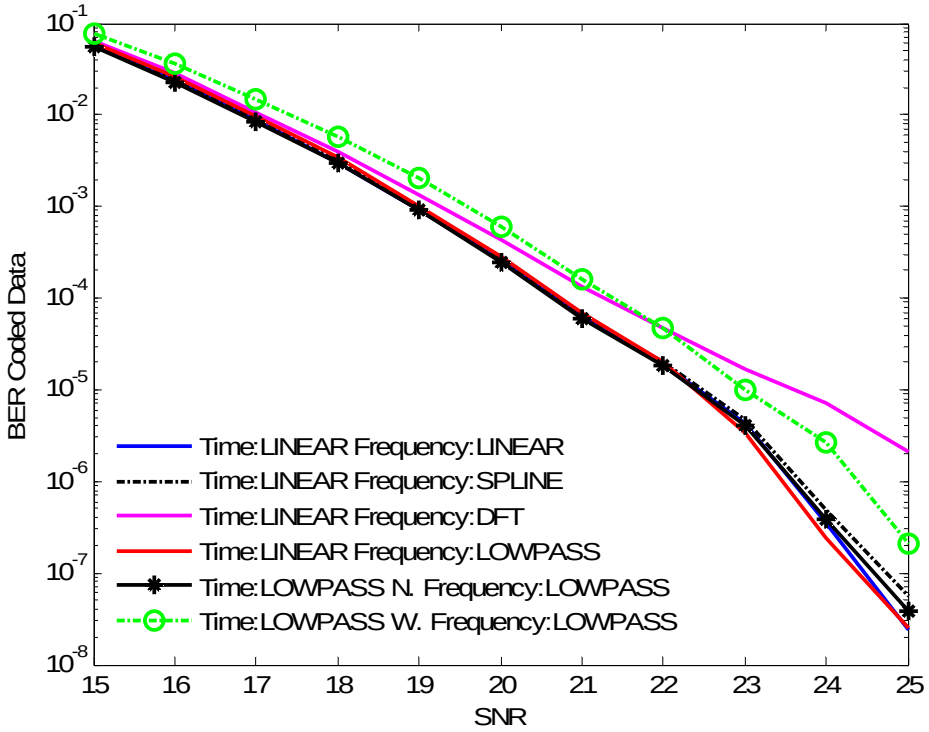

Figure 4.25: The BER of data after the Viterbi decoder for different interpolation algorithms. LMMSE estimation and MMSE4 channel equalization is used under Raleigh fading channel.

In Figure 4.25 coded BER performances are given for six types of interpolation algorithms for LMMSE channel estimation and MMSE4 channel equalization under Rayleigh fading channel. Both channel estimation and equalization algorithms optimize performance results so interpolators give same success. LMMSE mitigate the effects of noise linear and spline interpolation becomes better and achieved to the performances of low-pass interpolators.

Table 4.3: Required SNR for different interpolation algorithms and for different channel equalization methods to achieve BER=$2x10^{-4}$ after the Viterbi decoder. LMMSE channel estimation is used under Raleigh fading channel.

Required SNR(dB) for BER=$2x10^{-4}$ after Viterbi, QEF after Reed-Solomon	**Channel Estimation/ Equalization Method**	
Interpolation Algorithm Time/Frequency	LMMSE / ZF	LMMSE / MMSE4
Linear Time/Linear Frequency	*21.00*	*20.18*
Linear Time/Spline Frequency	*21.14*	*20.21*
Linear Time/DFT Frequency	*21.68*	*20.67*
Linear Time/Low-pass Frequency	*21.04*	*20.25*
Narrow Band Low-pass Time/ Low-pass Frequency	*21.23*	*20.13*
Wide Band Low-pass Time / Low-pass Frequency	*21.30*	*20.84*

Table 4.3 shows the required SNR results for QEF communication in the output of Reed-Solomon (RS) Decoder which is a BER of $2x10^{-4}$ at the Viterbi decoder output. For the same interpolation algorithms MMSE4 equalization has clearly better performances. The better approach for interpolation is low-pass, but linear time, linear frequency interpolation algorithms can also be considered because of simple implementation and minimizing storage memory.

In the following figures BER of data after Viterbi decoder for different interpolation algorithms. LS channel estimation and ZF channel equalization is used under fast fading Raleigh channel with 100Hz max Doppler shift.

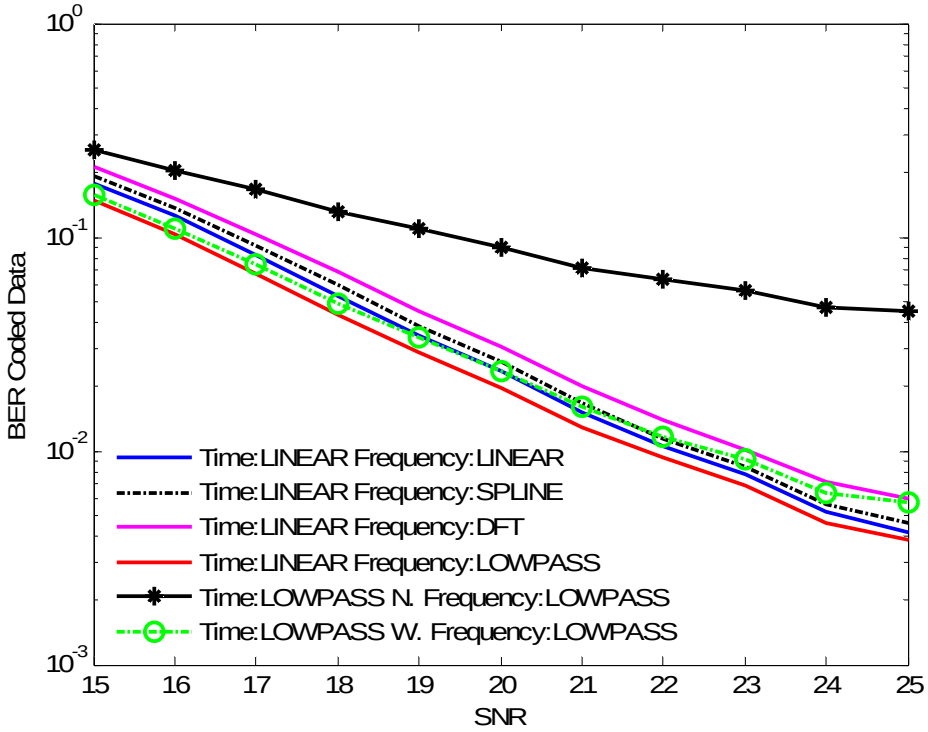

Figure 4.26: BER of data after Viterbi decoder for different interpolation algorithms. LS channel estimation and ZF channel equalization is used under fast fading Raleigh channel (100 Hz max Doppler shift).

In Figure 4.26 coded BER performances are given for six types of interpolation algorithms for LS channel estimation and ZF channel equalization under Rayleigh fading channel with max 100Hz Doppler Effect. Noise mitigation is depend on only interpolation, so low-pass interpolators performances can be higher, it is satisfied for linear time low-pass frequency interpolator but it is not satisfied for low-pass time and low-pass frequency interpolator because Doppler Effect highly influence in time direction so narrow band filter is not filtered the desired function any more, at this point wide band low-pass filter came across. When the frequency response of time direction CTF is effected from Doppler it shifts significantly so by using a wider low pass filter shifted will be still in the pass band of the filter. As shown Figure 4.26. wide-band filters performs better

than narrow-band filter but because of pass band region is wider performances is decreased for higher SNR according two linear time interpolators.

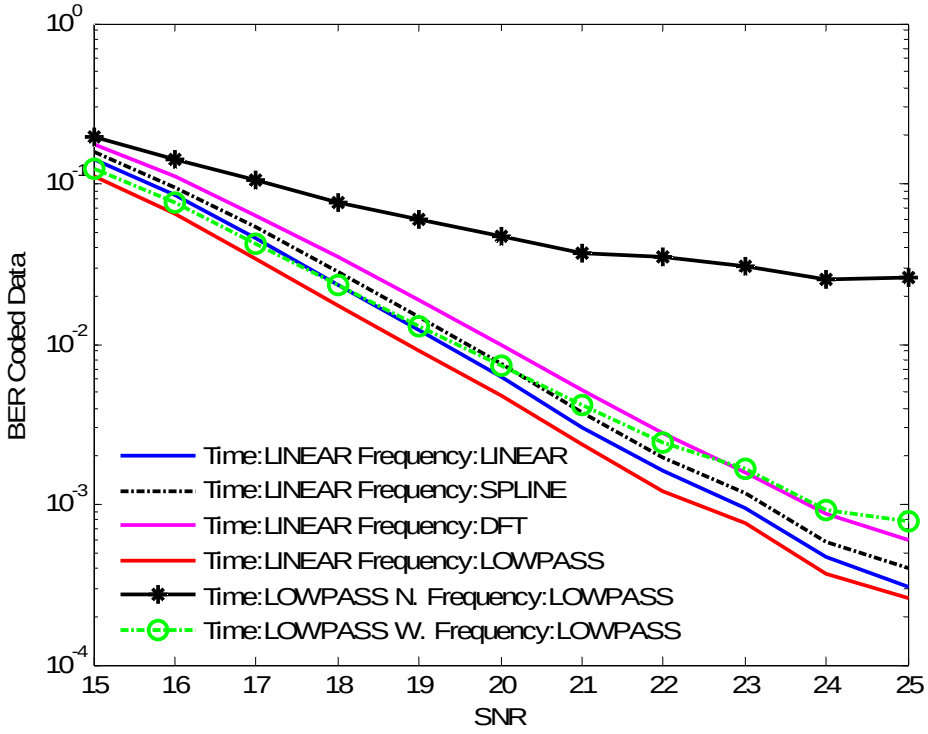

Figure 4.27: The BER of data after the Viterbi decoder for different interpolation algorithms. LS channel estimation and MMSE4 channel equalization is used under fast fading Raleigh channel(100Hz max Doppler shift).

In Figure 4.27 coded BER performances are given for six types of interpolation algorithms for LS channel estimation and MMSE4 channel equalization under Rayleigh fading channel with max 100Hz Doppler Effect. Noise mitigated by MMSE4 so performances all performances are better according to ZF channel equalization type but for low-pass interpolators same problem is stand still because of the Doppler as described in Figure 4.26.

4.4.1.1.3 Performance Analysis of Channel Estimation and Equalization

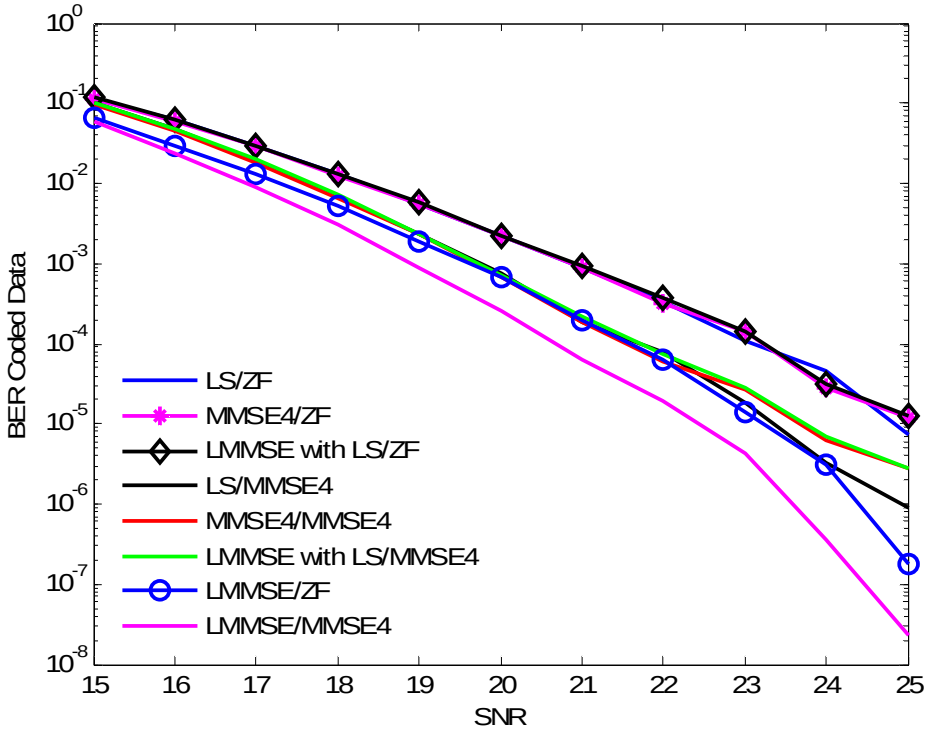

Figure 4.28: The BER of data after the Viterbi decoder for channel estimation and equalization methods. Linear time interpolation and linear frequency interpolation is used under Raleigh fading channel.

For linear time linear frequency interpolation the best channel equalization and estimation method is LMMSE/MMSE4, second method that can be considered is MMSE4 channel equalization and any channel estimation method.

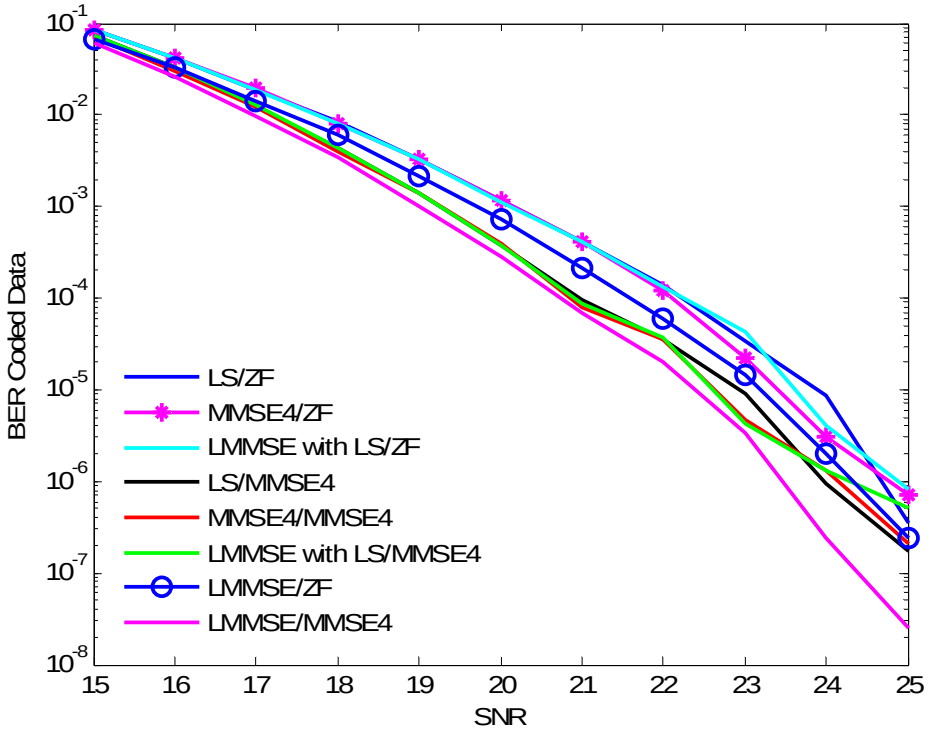

Figure 4.29: The BER of data after the Viterbi decoder for channel estimation and equalization methods. Linear time interpolation and low-pass frequency interpolation is used under Raleigh fading channel.

For linear time low-pass frequency interpolation the best channel equalization and estimation method is LMMSE/MMSE4, second method that can be considered is MMSE4 channel equalization and any channel estimation method.

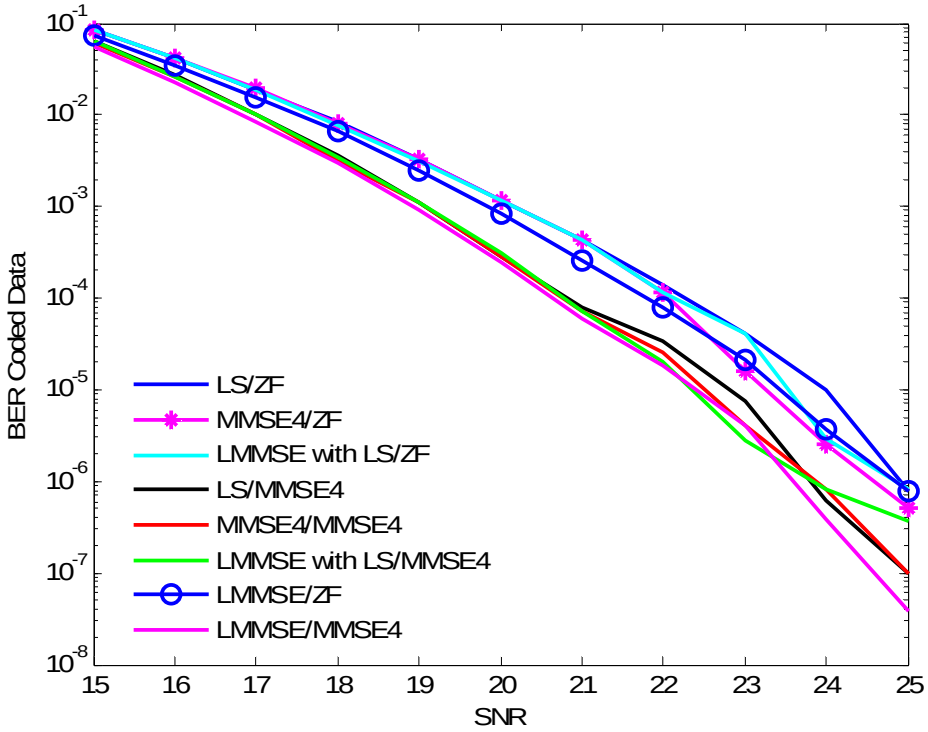

Figure 4.30: The BER of data after the Viterbi decoder for channel estimation and equalization methods. Low-pass with a narrow pass band time interpolation and low-pass frequency interpolation is used under Raleigh fading channel.

For narrow-band low-pass time low-pass frequency interpolation the best method is using channel equalization MMSE4 any channel estimation method.

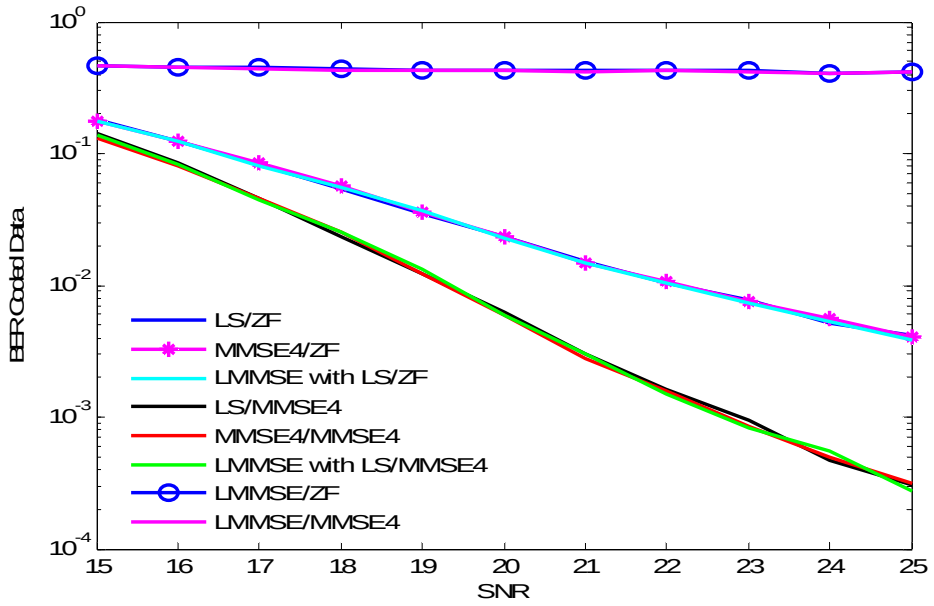

Figure 4.31: The BER of data after the Viterbi decoder for channel estimation and equalization methods. Linear time interpolation and linear frequency interpolation is used under fast fading Raleigh channel (100Hz max Doppler shift).

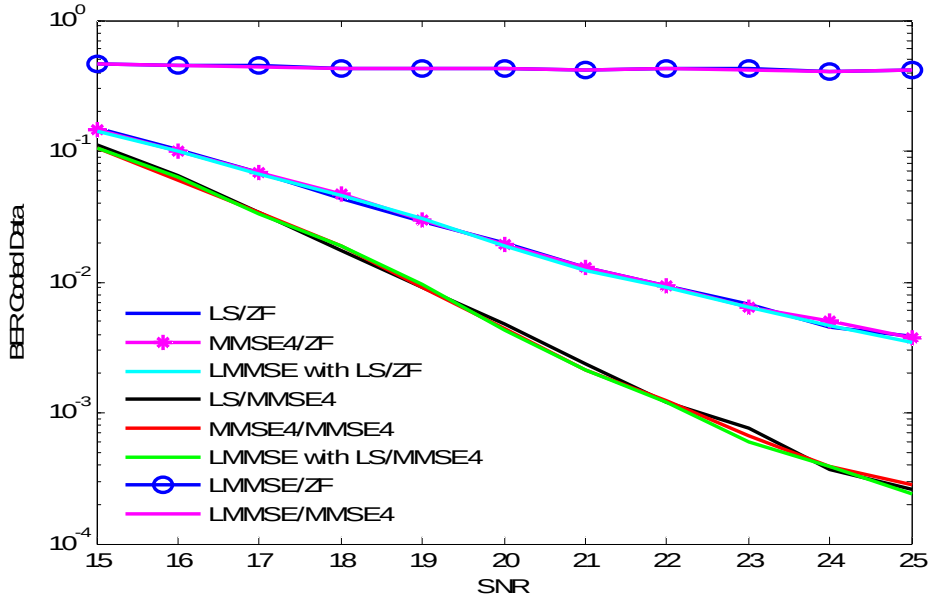

Figure 4.32: The BER of data after the Viterbi decoder for channel estimation and equalization methods. Linear time interpolation and low-pass frequency interpolation is used fast fading Raleigh channel (100Hz max Doppler shift).

In Figure 4.31 For the Doppler Effect case using linear time linear frequency interpolation the best channel equalization method is MMSE4 with all channel estimation algorithms except LMMSE because it is vulnerable to Doppler effect. For channel equalization MMSE4 is not only the best solution for noise reduction it is also the best way to cope with Doppler Effect.

Figure 4.32 For the Doppler Effect case using linear time low-pass frequency interpolation the best channel equalization method is MMSE4 with all channel estimation algorithms except LMMSE because it is vulnerable to Doppler effect. For channel equalization MMSE4 is not only the best solution for noise reduction it is also the best way to cope with Doppler Effect.

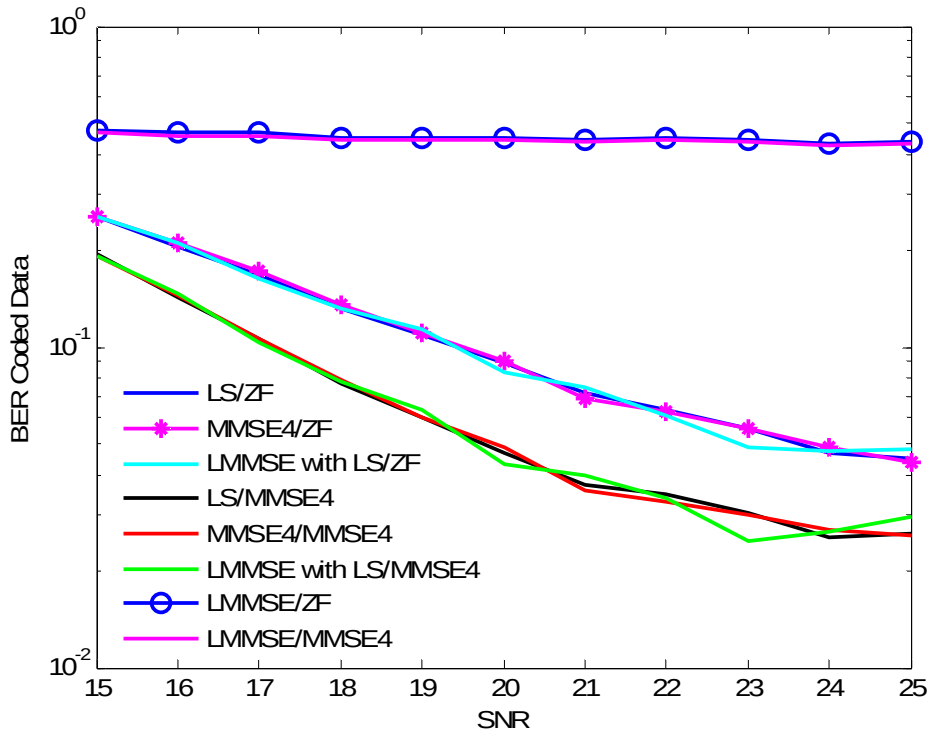

Figure 4.33: The BER of data after the Viterbi decoder for channel estimation and equalization methods. Low-pass with a narrow pass band time interpolation and low-pass frequency interpolation is used fast fading Raleigh channel (100Hz max Doppler shift).

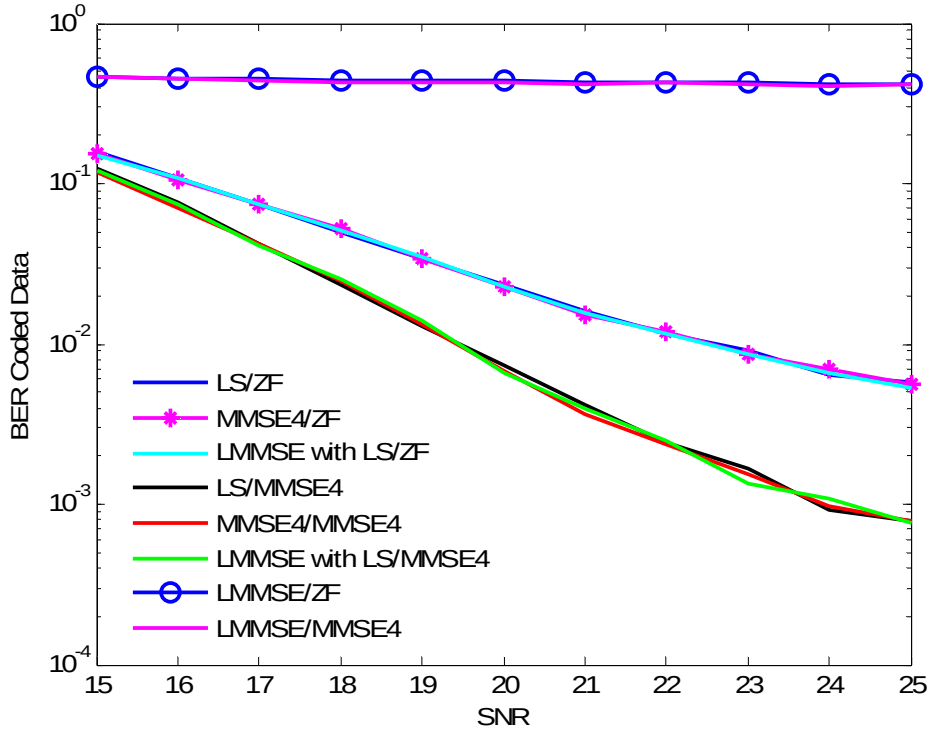

Figure 4.34: The BER of data after the Viterbi decoder for channel estimation and equalization methods. Low-pass with a wide pass band time interpolation and low-pass frequency interpolation is used under fast fading Raleigh channel (100Hz max Doppler shift).

In Figure 4.33 for the Doppler Effect case using low-pass with a narrow pass band time low-pass frequency interpolation the best channel equalization method is MMSE4 with all channel estimation algorithms except LMMSE because it is vulnerable to Doppler effect. The overall solution for narrow band low pass interpolation has poor performances so it cannot be used by Doppler Effect.

In Figure 4.34 for the Doppler Effect case using low-pass with a wide pas-band time low-pass frequency interpolation the best channel equalization method is MMSE4 with all channel estimation algorithms except LMMSE because it is

vulnerable to Doppler effect. The overall solution for wide-band clearly has better performances according to narrow band low pass interpolation.

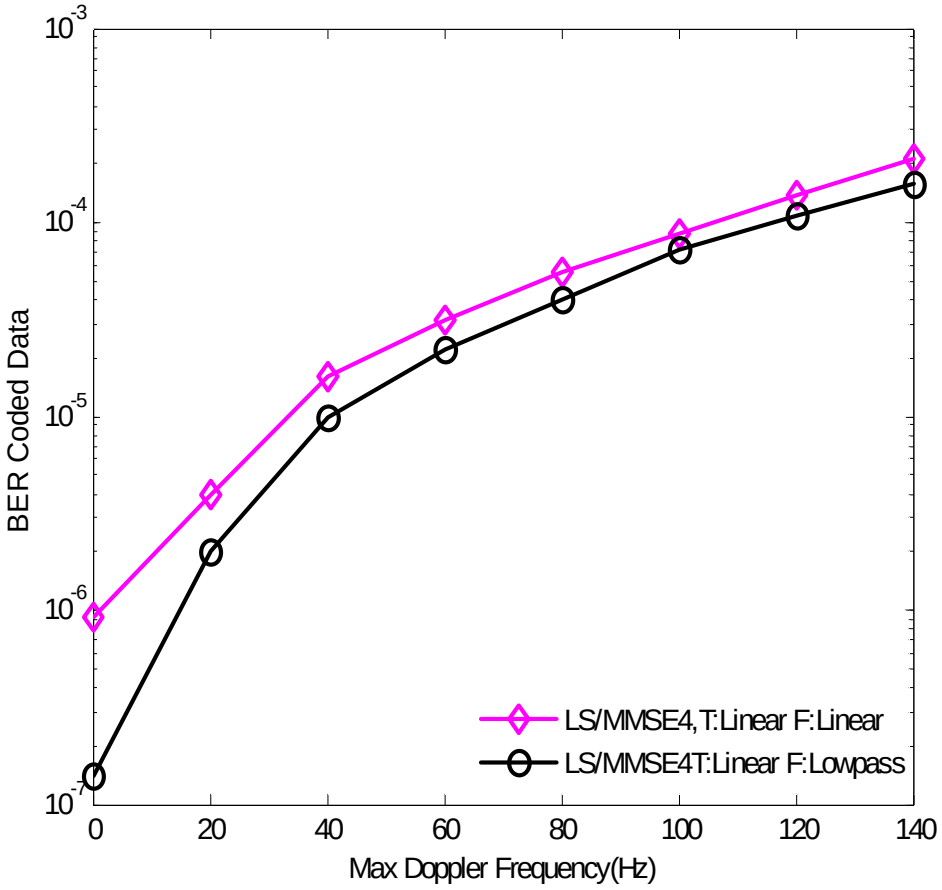

Figure 4.35: The BER of data after the Viterbi decoder for same linear time interpolation vs. two frequency interpolations linear and low-pass to different values of max Doppler Frequency shifts. LS/MMSE4 channel estimation and equalization is used.(SNR=20dB) and Rayleigh fading channel is used.

4.4.1.1.4 Performance Comparisons of Channel Estimation and Equalization

In the following table the system performances are compared with the values in ETSI 300 744 V1.5.1 (For perfect channel estimation and no noise amplification assumption case) [1].

Table 4.4: Required C/N ratio to achieve a BER = $2X10^{-4}$after the Viterbi decoder Vs. The simulated performances(Perfect channel astimation is assumed)

		Required C/N for BER =2x10-4 after Viterbi QEF after Reed-Solomon Vlues taken from ETSI 300 744 V.1.5.1 and simulation results of DVB-T System						
Mapping	Code Rate	ETSI Gaussian Channel	DVB-T System Gaussian Channel	ETSI Ricean Channel	DVB-T System Rician Channel	ETSI Rayleigh Channel	DVB-T System Rayleigh Channel	Bitrate (Mbits/s)
QPSK	1/2	3.1	3.0	3.6	4	5.4	6	4.98
QPSK	2/3	4.9	4.9	5.7	5.8	8.4	9.5	6.64
QPSK	3/4	5.9	6.0	6.8	7.0	10.7	11.4	7.46
16-QAM	1/2	8.8	9.0	9.6	10.0	11.2	12	9.95
16-QAM	2/3	11.1	11.2	11.6	12.0	14.2	15	13.27
16-QAM	3/4	12.5	12.7	13.0	13.0	16.7	17.4	14.93
64-QAM	1/2	14.4	14.7	14.7	15.0	16.0	17	22.3
64-QAM	2/3	16.5	16.9	17.1	17.3	19.3	21	19.3
64-QAM	3/4	18.0	18.4	18.6	19.0	21.7	22.5	21.1

This test is proven that the coding performance of our DVB-T system has similar values with the one in the standard.

4.4.1.1.5 Performance Analysis of Interleaving

The DVB-T standard specifies a combination of bit and symbol inner interleaving as mentioned in the second chapter. In the following figures interleaving performances are given for symbol and bit interleaving and no interleaving cases in terms of SNR and coded BER. For symbol recovery LS channel estimation using linear time-linear frequency interpolation with MMSE4 channel equalization is used. Results are compared with the given literature [38].

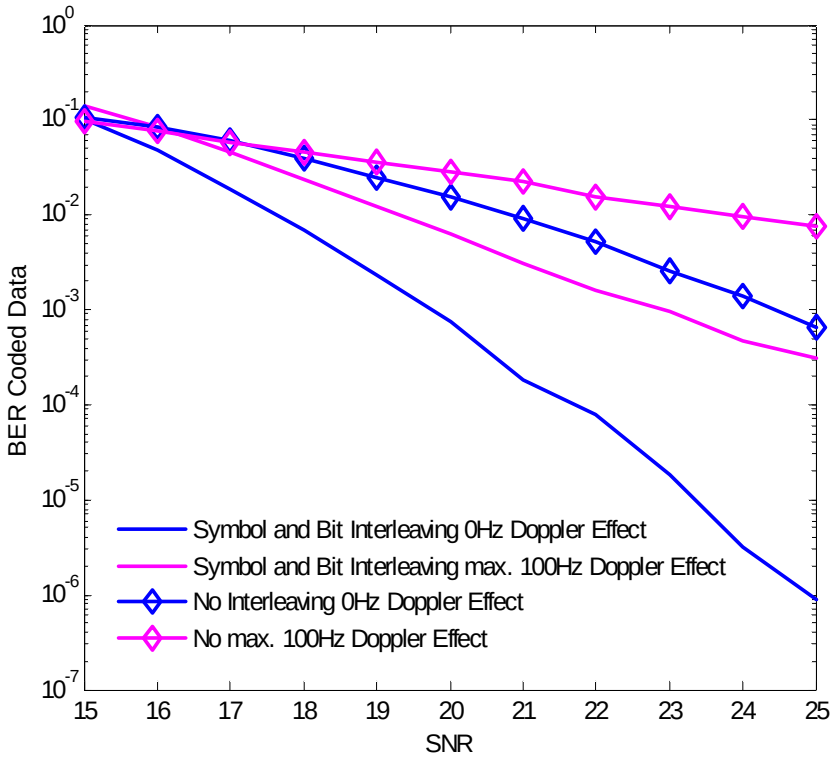

Figure 4.36: The BER of data after the Viterbi decoder for symbol and bit interleaving vs. no interleaving is given. LS channel estimation linear time-linear frequency interpolations and MMSE4 channel equalization is used under Rayleigh fading channel with Doppler Effect.

4.4.1.1.6 Performance Analysis of Power of Pilot Sub-Carriers

Pilot sub-carriers are inserted in the OFDM frame for channel estimation purposes. The power of the pilots can be varied with respect to information carried sub carriers in order to reduce estimation and equalization error and similar results are obtained with [38].

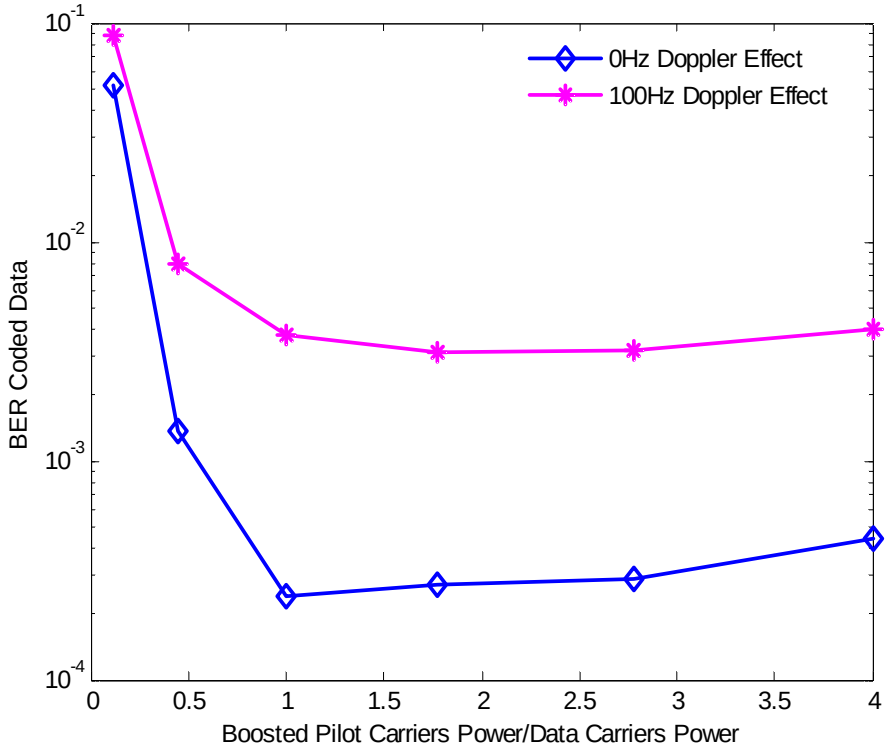

Figure 4.37: The BER of data after the Viterbi decoder for pilot carriers power to data carriers power ratio. LS channel estimation linear time-linear frequency interpolations and MMSE4 channel equalization is used under Rayleigh fading channel with Doppler Effect.

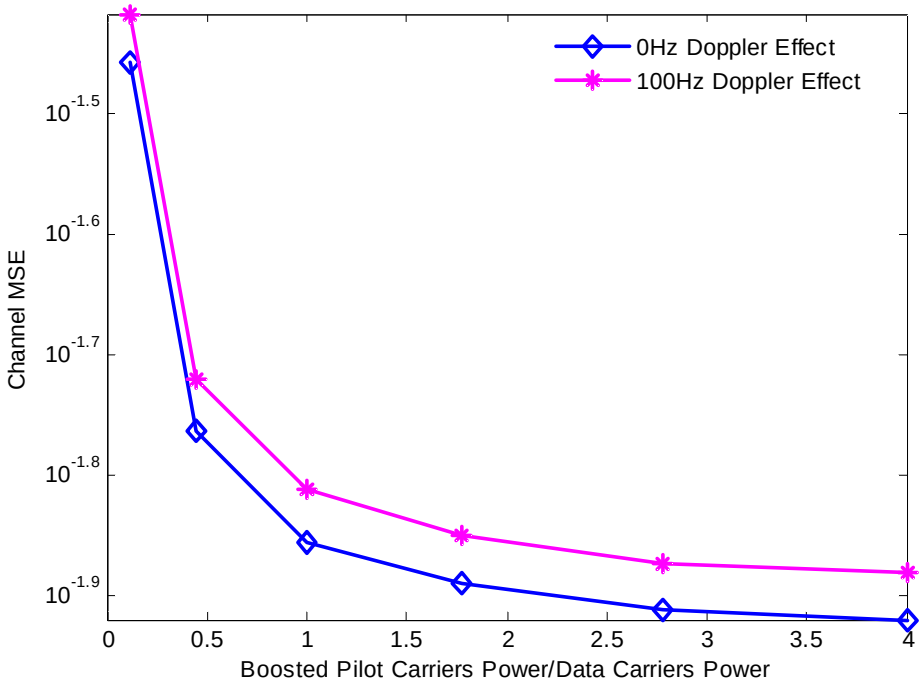

Figure 4.38: The channel MSE for pilot carriers power to data carriers power ratio. LS channel estimation linear time-linear frequency interpolations and MMSE4 channel equalization is used under Rayleigh fading channel with Doppler Effect.

4.4.1.1.7 Performance Analysis Viterbi Decoder Demodulation Resolution

The number of quantization level is one of the important parameters in Viterbi Decoding. The following figure shows the BER for different values of demodulation resolution bit.

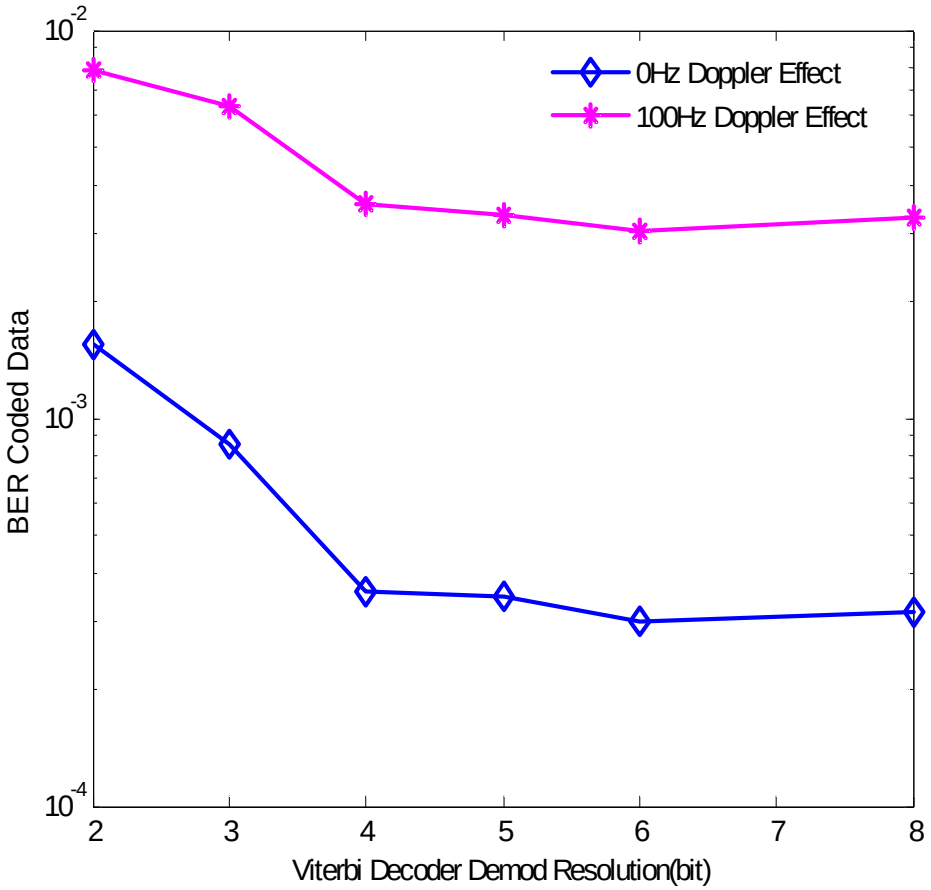

Figure 4.39: BER of data after Viterbi decoder for Viterbi decoder's demod resolution performances. The channel MSE for pilot carriers power to data carriers power ratio. LS channel estimation linear time-linear frequency interpolations and MMSE4 channel equalization is used under Rayleigh fading channel with Doppler Effect.

The main important parameter of Viterbi s the number soft decision bits. Increasing soft decision bit number improves the error-correction capability. As shown in Figure 4.39 and a resolution higher than 4 is a hardly improvement and only increase the implementation requirement similar results are obtained in [36], [37], [38].

CHAPTER 5

FRAME SYNCHRONIZATION

5.1 INTRODUCTION

In typical communication systems one of the main problems is to detect a frame with correct timing in the received signal to accomplish coding, block processing etc. The primary source of the problem is the unknown symbol arrival time. For estimating the proper time instant to start processing a new frame and compensate framing error, frame synchronization must be performed. In this chapter we investigate Maximum Likelihood (ML) Frame Synchronization technique [21], [39], [40] and [41] which is applied to OFDM and also performed in simulations.

Sensitivity to frame timing is higher in multicarrier systems than in single carrier systems. In OFDM, the key element is that, the OFDM data symbols already contain necessary information in order to choose the true starting point of the OFDM window.

It is necessary to consider the OFDM frame (symbol) structure in order to investigate the frame synchronization. OFDM complex data symbols are modulated using IDFT on N-parallel sub-carriers which form an OFDM symbol. The last samples from one IDFT symbol are copied to the beginning of the same IDFT symbol. At the receiver side the receiver discards the beginning part of the received symbol. As mentioned in the previous chapters these copied symbols are called cyclic prefix.

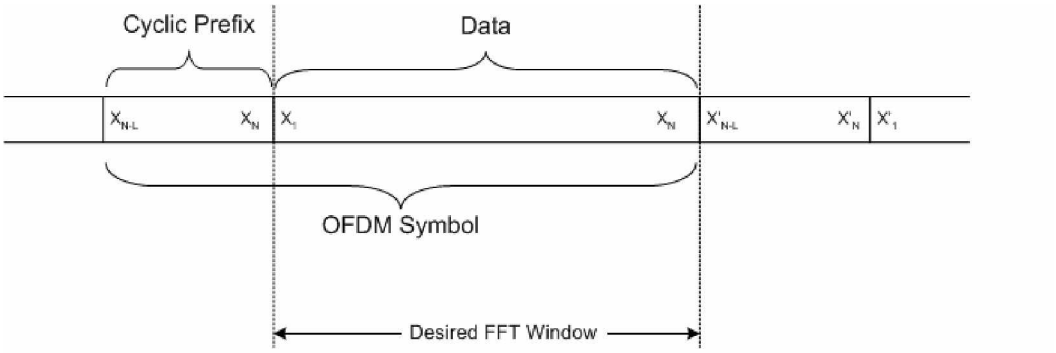

Figure 5.1 OFDM symbol structure

This OFDM symbol is serially transmitted over a channel, whose impulse response is shorter than cyclic prefix size (L samples). We use this cyclic prefix to perform frame synchronization. The effective length of OFDM symbol is $N+L=M$ long where N is the number of sub-carriers and defines the length of the desired FFT window For the synchronization concept the number of sub-carriers N and the length of the cyclic prefix L are important parameters. They describe the amount of redundancy in the signal that the estimator can exploit.

These OFDM symbol structure is given in Figure 5.1. Considering this structure the desired FFT window must be chosen with correct timing in order to prevent framing error as shown in Figure 5.1. So as a result of frame synchronization a FFT window is defined.

In the following part the Maximum Likelihood (ML) Frame Synchronization technique is discussed.

5.2 Maximum Likelihood (ML) Frame Synchronization

The key element of the ML estimation depends on the periodicity of the preceding OFDM symbols which accomplished by cyclic prefix usage. ML estimation uses the cyclic prefix in order to synchronize frames so by using this

redundant information carried in cyclic prefix, additional pilots are not needed to be used [40].

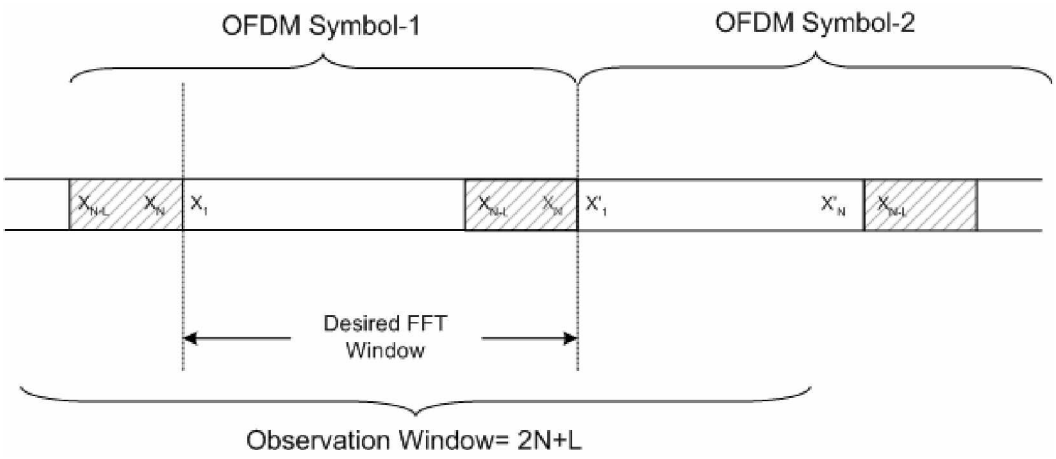

Figure 5.2 OFDM Frame synchronization

In Figure 5.2 observation window of the frame synchronization process is shown. By using a window with length 2N+1 it guaranteed that the frame synchronization process can utilize the N+L long OFDM symbol which includes cyclic prefix and data. In other word this observation window contains the necessary information for synchronization; however the position of this symbol within the observed block of samples is unknown because the channel delay is unknown to the receiver.

Assume the channel is non dispersive and the transmitted signal *u(k)* is only affected by the complex additive white Gaussian noise (AWGN) *n(k)*. The main uncertainties in the receiver are the arrival time of the OFDM symbol and the uncertainty in the carrier frequency offset. These uncertainties are modeled as in [40]

$$y(k) = u(k-\theta)e^{j2\pi\varepsilon(k/N)} \tag{5.1}$$

where θ is the sampling time offset and ε is the carrier frequency offset. We know that 2 part of L samples (I and I') with a distance of N samples are same, because of cyclic prefix usage and only differs with a noise factor.

The correlation relation of this two parts (I and I') is:

$$\forall k \in I : E\{y(k)y^*(k+m)\} = \begin{cases} \sigma_y^2 + \sigma_n^2 & m = 0 \\ \sigma_y^2 e^{-j2\pi\varepsilon}, & m = N \\ 0, & otherwise \end{cases} \quad (5.2)$$

Where, $\sigma_n^2 = E\{n(k)^2\}$ and $\sigma_y^2 = E\{y(k)^2\}$ besides the remaining symbols ($r(k) \notin I \cup I'$) are mutually uncorrelated.

The log-likelihood function for θ and ε; Λ(θ, ε) is simply the logarithm of the probability density function of the 2N+L observed samples in r given the time 'θ' the carrier frequency offset 'ε'

$$\Lambda(\theta,\varepsilon) = \log f(r|\theta,\varepsilon) \quad (5.3)$$

For θ and ε this log-likelihood function is derived as [40]

$$\Lambda(\theta,\varepsilon) = |\gamma(\theta)|\cos(2\pi\varepsilon + \angle\gamma(\theta)) - \rho\Phi(\theta) \quad (5.4)$$

where, $\gamma(m)$ and $\Phi(m)$ represent:

$$\gamma(m) = \sum_{k=m}^{m+M-1} y(k)y^*(k+N) \quad (5.5)$$

$$\Phi(m) = \frac{1}{2} \sum_{k=m}^{m+M-1} \left|y(k)\right|^2 + \left|y(k+N)\right|^2 \tag{5.6}$$

$$\rho = \left| \frac{E\left\{y(k)y^*(k+N)\right\}}{\sqrt{E\left\{\left|y(k)\right|^2\right\}E\left\{\left|y(k+N)\right|^2\right\}}} \right| = \frac{\sigma_y^2}{\sigma_y^2 + \sigma_n^2} = \frac{SNR}{SNR+1} \tag{5.7}$$

When the joint ML estimation is done [40] we have

$$\hat{\varepsilon}_{ML}(\theta) = -\frac{1}{2}\angle\gamma(\theta) \tag{5.8}$$

$$\hat{\theta}_{ML} = \arg\max_{\theta}\left\{\left|\gamma(\theta)\right| - \rho\Phi(\theta)\right\} \tag{5.9}$$

A maximum of the joint ML estimation $\hat{\theta}_{ML}$ gives the time offset so we can find frame start position.

However, due to the channel delay spread and noise exact frame start position may not be found. If the ML estimation finds the symbol start position in the cyclic prefix hence there is no ISI in this region we do not lose data but the only effect is the rotation of data in the FFT window.

Assume that $y(t) = u(t)*h(t) + n(t)$ if we find the ideal FFT window

$Y(k) = U(k)H(k) + N(k)$ and if there is a ϕ shift from ideal FFT window, we have

$Y(k) = U(k)H(k)e^{-j2\pi k\phi/N} + N(k)$ [40]. In channel estimator this phase effect can be seen as a multiply of channel response so can be compensated in the channel equalization block.

As a result by utilizing the property of the fact that cyclic prefix repeats in the observation window length 2N+L, the frame synchronization is accomplished.

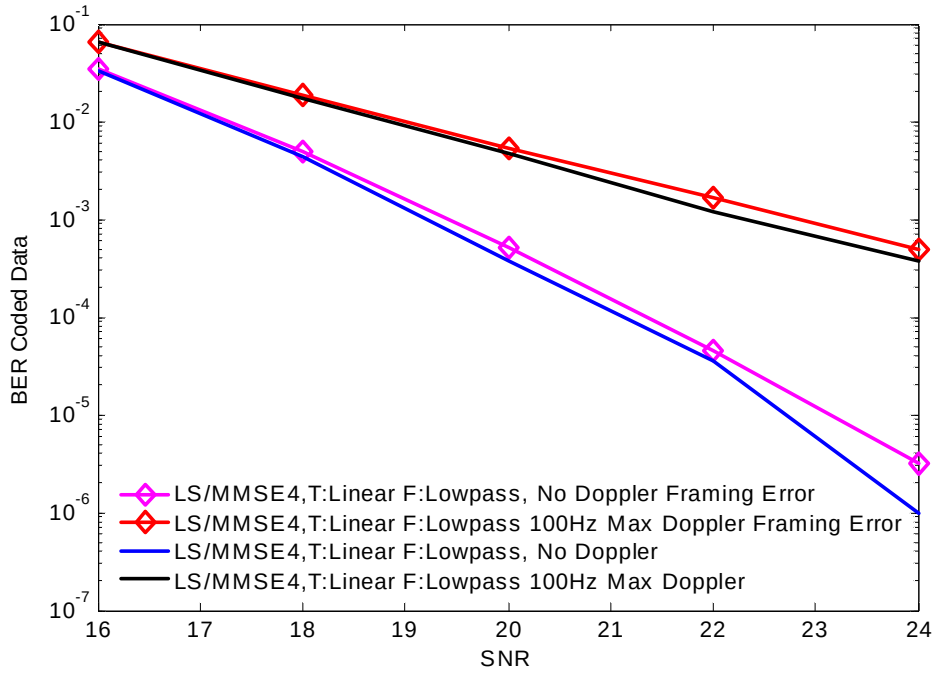

Figure 5.3: The BER of data after the Viterbi decoder for random framing error using LS channel estimation, MMSE4 channel equalization and linear time, low-pass frequency interpolation.

In table 5.1, Frame synchronization errors vs. SNR and maximum Doppler shift, are given the values are in terms of difference index value from the original start position and the estimated one. Same transmitter and receiver signal properties and channel properties as in figure 3.1 except random framing error.

Table 5.1: Frame synchronization errors vs. SNR and maximum Doppler shift, are given the values are in terms of difference index value.

SNR(dB)	16	18	20	22	24	26
LS/MMSE4 Channel Estimation and Equalization Linear Time Low-pass Frequency interpolation	2.8	2.6	2.2	2.2	2.3	2.2
LS/MMSE4 Channel Estimation and Equalization Linear Time Linear Frequency interpolation	3.1	3.1	3	3	2.9	2.7
LS/MMSE4 Channel Estimation and Equalization Linear Time Low-pass Frequency interpolation	5.1	5.2	5	4.6	4.2	4.2
LS/MMSE4 Channel Estimation and Equalization Linear Time Linear Frequency interpolation	5.3	5.1	5.3	48	4.5	4.4

CHAPTER 6

CONCLUSION

In this thesis the standard of ETSI EN 300 744 for Terrestrial Digital Video Broadcasting is implemented. All the functional blocks of DVB-T transmit and receive system is reviewed in detail including, error correction coding and decoding, OFDM transmission, frame synchronization, channel estimation and channel equalization. According to performance specifications of these functional block a base-band receiver for 2k mode non hierarchical DVB-T is implemented. As a part of DVB-T receiver various channel estimation and equalization methods and ML frame synchronization method are investigated and implemented. After that for different wireless broadcast impairments such as multipath fading, additive noise, Doppler Effect, symbol interference and framing error the performances of the complete system have been evaluated.

After a detail survey on channel estimation four types of channel estimation method is adopted to DVB-T system which are least square (LS) estimation, linear minimum mean-square error (LMMSE) estimation with known channel transfer function, linear minimum mean-square error estimation with utilizing the result of LS estimation and minimum mean square error (MMSE) estimation with the assumption of noise to be white and its variance is known.

As a part of channel estimation process various types of interpolation techniques are investigated and implemented such as; linear, low pass, Spline, DFT interpolation.

For equalizing the received signal two types of channel equalization methods are modified to the DVB-T system which are zero forcing (ZF) and minimum mean-square error (MMSE).

The maximum likelihood frame synchronization method are also investigated and adopted to the system for analyzing the effect frame synchronization error.

The channel equalization and estimation performances are evaluated for Rayleigh multipath fading channel with Doppler Effect. The performance results are given in the means of channel minimum mean square error (MSE) and coded bit error rate (BER).

Based on simulation results it is shown that MMSE equalizer has better performances in channel equalization when comparing to ZF equalizer because ZF equalizer is more susceptible to noise.

Although the LMMSE estimation state the best channel estimation performances for no Doppler Effect case it has the highest computational complexity and also to perform LMMSE real channel response has to be known. When using Doppler Effect it gives the worst performance results because the actual Doppler properties which change channel response is unknown.

When dealing with 2D time-frequency interpolation algorithms the better solution is low-pass interpolation for no Doppler Effect case. When Doppler Effect is added the better interpolation is became linear in time direction and low-pass in frequency direction. Also the performance of linear time direction and linear frequency direction interpolator gives a good approximation with MMSE channel equalization, while maintaining low complexity and minimizing storage delay in the receiver.

The results of performance analysis for channel estimation and equalization using Rayleigh multipath fading with Doppler Effect shows that: For the coded BER, estimating channel using different algorithms is not improves the

performances much, the improvement is satisfied by only decreasing noise effects. DVB-T pilot configuration and power allocation of pilot symbols is chosen efficient in standard so channel estimation is not a crucial problem when using the investigated algorithms. The system performances is increased by noise compensation which performed better using low-pass interpolations, MMSE channel equalization and for Doppler Effect free case LMMSE channel estimation.

We proposed that for DVB-T transmission if there are two important problems to cope with which are estimating channel transfer function and mitigate the effect of noise the crucial point is noise effect because DVB-T pilot arrangement is already deal with estimating channel transfer function efficiently. If noise mitigation will be a hard issue, design of channel estimation and equalization methods which uses blind algorithms seems to be hot topic to increase transmitted bit rate where no pilot symbols are used in DVB-T OFDM research.

REFERENCES

[1] "Digital Video Broadcasting (DVB); Framing structure, channel coding and modulation for digital terrestrial television", ETSI EN 300 744 v1.5.1 (2004-11), 2004.

[2] U. Riemers, "Digital Video Broadcasting, The International standard for Digital Television", Springer—Verlang Berlin Heildeberger, New York, 2001.

[3] DVB Project, "Transmission Systems for Handheld Terminals (DVB-H)", DVB document A081, June 2004.

[4] DVB Project, "Digital Video Broadcasting (DVB); Interaction channel for Digital Terrestrial Television (DVB-RCT) incorporating Multiple Access OFDM", DVB-TM document TM2361r3, March 2001 and ETSI, EN 301 958 DVB-RCT standard, 2001.

[5] S. B. Weinstein, P. M. Ebert, "Data Transmission of Frequency Division Multiplexing Using The Discrete Frequency Transform", IEEE Transactions on Communications, COM-19(5), pp. 623-634, October 1971.

[6] J. A. C. Bingham, "Multi-carrier modulation for data transmission: An idea whose time has come", IEEE Communication Magazine, vol. 28, no. 5, pp. 5-14, May 1990.

[7] Ove Edfors, Magnus Sandell, Jan-Jaap van de Beek, Daniel Landstrom, Frank Sjoberg, "An Introduction to orthogonal frequency division multiplexing" University of Lulea, September,1996

[8] R.V. Nee, R. Prasad, “OFDM for Wireless Multimedia Communications”, Artech House Publishers, 2000.

[9] E. P. Lawrey, “Adaptive Techniques for Multi-user OFDM,” Ph.D. thesis, James Cook University, Australia, December 2001.

[10] B. R. Saltzberg, “Performance of an Efficient Parallel Data Transmission System”, IEEE Transactions on Communications, COM-15 (6), pp. 805-811, December 1967.

[11] R. Peled, A. Ruiz, “Frequency Domain Data Transmission Using Reduced Computational Complexity Algorithms”, in Proceeding of the IEEE International Conference on Acoustics, Speech, and Signal Processing, ICASSP’80, pp. 964-967, Denver, USA, 1980.

[12] M. I. Rahman, S. S. Das, F. H. P. Fitzek, “OFDM Based WLAN Systems”, Technical Report R-04-1002; v1.2, Aalborg University, February 2005

[13] C. R. Nassar, Multi-carrier Technologies for Wireless Communication, Kluwer Academic Publishers, 2002.

[14] Wireless Data Communications, “High Speed Wireless OFDM Communication Systems”, whitepaper, Wi-LAN Inc., February 2001.

[15] A. R. S. Bahai, B. R. Satzberg, “Multi-Carrier Digital Communications: Theory and Applications of OFDM”, Kluwer Academic/Plenum Publishing NY 1999.

[16] J. Kim, J. Park, D. Hong, "Performance Analysis of Channel Estimation in OFDM Systems", IEEE Signal Processing Letters, Vol. 12, No. 1. January 2005.

[17] M. H. Hsieh, C. H. Wei, "Channel Estimation for OFDM Systems Based on Comb-Type Pilot Arrangement in Frequency Selective Fading

Channels", IEEE Transactions on Communications, Vol. 44, no.1, pp. 217-225, February 1998.

[18] S. Coleri, M. Ergen, A. Puri, and A. Bahari, “Channel Estimation Techniques Based on Pilot Arrangement in OFDM System”, IEEE Transactions on Broadcasting, vol. 48, no. 3, pp. 223-229, September 2002.

[19] X. Wang, Y. Wu, J. Y. Chouniard, S. Lu, B. Caron, “A Channel Characterization Technique Using Frequency Domain Pilot Time Domain Correlation Method for DVB-T Systems”, IEEE Transactions on Consumer Electronics, vol. 49, no. 4, pp. 949-957, November 2003.

[20] F. Frescura, S. Pielmeier, G. Reali, G. Baruffa, S. Cacopardi, "DSP Based OFDM Demodulator and Equalizer for Professional DVB-T Receivers", IEEE Transactions on Broadcasting, vol.45, no. 3, pp. 323- 332, December 1999.

[21] S. H. Chen, W. H. He, H. S. Chen, and Y. Lee, “Mode Detection, Synchronization, and Channel Estimation for DVB-T OFDM Receiver”, Globecom 2003 Conference, August 2003.

[22] A. A. Hutter , R. Hasholzner, J. S. Hammerschmidt, "Channel Estimation for Mobile OFDM Systems", IEEE International Vehicular Technology Conference , 1999.

[23] O. Edfors, M. Sandell, J. J. Beek, S. K. Wilson, P. O. Börjesson, "OFDM Channel Estimation by Singular Value Decomposition", IEEE Transactions on Communications, vol. 46, no.7, pp. 931-939 July 1998.

[24] R. Steele, Mobile Radio Communications, London, England, Pentech Press Limited, 1992.

[25] U. Reimers, “Digital Video Broadcasting,” IEEE Communication Magazine, vol. 36, no.6, pp.104-110, June 1998.

[26] J. J. van de Beek, O. Edfors, M. Sandell, S. K. Wilson, P. O. Börjesson, " On Channel Estimation in OFDM Systems ", in Proc. IEEE 45th Vehicular Technology Conference, Chicago, IL, USA, July 1995, pp.815-819.

[27] Y. Zeng, T. S. Ng, "Pilot Cyclic Prefixed Single Carrier Communication: Channel Estimation and Equalization", IEEE Signal Processing Letters, vol. 12, no. 1, pp. 56-59 January 2005.

[28] H. Sarı, G. Karam, I. Jeanclaude, "Transmission Techniques for Digital Terrestrial TV Broadcasting", IEEE Communication Magazine, pp. 100-109, Februrary 1995.

[29] Oppenheim, A.V., and R.W. Schafer, Discrete-Time Signal Processing, Prentice-Hall, Englewood Cliffs, NJ, 1989, pp. 256-266.

[30] M. Garcia, J. Boralllo, S. Zazo, "DFT-based Channel Estimation in 2D-Pilot-Symbol-Aided OFMD Wireless Systems", IEEE Proceedings of VTC'01, pp.810-814, 2001

[31] F. Tufvesson, T. Maseng, "Pilot Assisted Channel Estimation for OFDM In Mobile Cellular Systems", IEEE Proceedings of VTC'97, pp. 1639-1643, March 1997.

[32] A. Dowler, A. Doufexi, A. Nix, "Performance Evaluation of Channel Estimation Techniques for a Mobile Fourth Generation Wide Area OFDM System", IEEE Proceedings of VTC'02, pp. 2036-2040, March 2002.

[33] M. Speth, S. Fechtel, G. Fock, H. Meyr, "Broadband Transmission Using OFDM: System Performance and Receiver Complexity", IEEE Proceedings of VTC'98, pp. 99-104, June 1998.

[34] Programs for Digital Signal Processing, IEEE Press, New York, 1979, Algorithm 8.1.

[35] Oppenheim, A.V., and R.W. Schafer, Discrete-Time Signal Processing, Prentice-Hall, Englewood Cliffs, NJ, 1989.

[36] A. G. Armada, B. Bardon, M. Calvo, "Parameter Optimization and Simulated Performance of a DVB-T Digital Television Broadcasting System", IEEE Transactions on Broadcasting, Vol. 44, No. 1, March 1998.

[37] K. M. Lee, D. S. Han, K. B. Kim, "Performance of the Viterbi Decoder for DVB-T in Rayleigh Fading Channels", IEEE Transactions on Consumer Electronics, Vol. 44, No. 3, August 1998.

[38] T. Kratochvil, "Digital Video Broadcasting Channel Encoding and Decoding Simulation", 4th EURASIP Conference, 2003.

[39] J. J. Beek, M. Sandell, M. Isaksson, P. O. Börjesson, "Low-Complex Frame Synchronization in OFDM Systems" IEEE Proceedings of VTC'95, pp. 982-986, April 1995.

[40] J. J. van de Beek, M. Sandell, P. O. Börjesson, "ML Estimation of Time and Frequency Offset in OFDM Systems", IEEE Transactions on Signal Processing, vol. 45, no. 7, July 1997.

[41] H. Y. Gürsan, "Frame Synchronization in OFDM Systems", M. Sc. Thesis, METU, January 2005.